Advanced Sensor and Energy Materials 4 (2025) 100139

Contents lists available at ScienceDirect

Advanced Sensor and Energy Materials

journal homepage: www.sciencedirect.com/journal/advanced-sensor-and-energy-materials

Review

3D-printed microneedles for sensing applications: Emerging topics and future trends

Kelcilene B.R. Teodoro [a,*], Tamires S. Pereira [a,b], Ana Laura M.M. Alves [a,b], Francisco V. dos Santos [a,c], Fabrício A. dos Santos [a], Daniel S. Correa [a,b,c,**]

[a] Nanotechnology National Laboratory for Agriculture (LNNA), Embrapa Instrumentação, São Carlos 13560-970, SP, Brazil
[b] PPGQ, Department of Chemistry, Center for Exact Sciences and Technology, Federal University of São Carlos (UFSCar), 13565-905 São Carlos, SP, Brazil
[c] PGrCEM, Department of Materials Engineering, São Carlos School of Engineering, University of São Paulo, São Carlos 13563-120, SP, Brazil

A R T I C L E I N F O

Keywords:
3D-assembling
Additive manufacturing
Transdermal monitoring
Point-of-care
Microfabrication
Sensor
Biosensor

A B S T R A C T

3D-printed microneedles (MNs) have revolutionized the biomedical sector, enabling applications in aesthetic treatments, vaccine delivery, diagnostics, and real-time biomarker analysis. These minimally invasive structures advance the development of sensors and biosensors for diverse applications, including human, veterinary, agricultural, and environmental domains. Recent trends favor MNs made from polymers and nanomaterials over traditional metals, addressing challenges related to cost, biocompatibility, and scalability. In this context, this review explores recent advancements on different MNs-based sensors, fabricated by 3D printing, highlighting innovations, shortcomings and also pointing future opportunities to expand their applications in medical, agricultural and environmental domains. Initially, we discuss the general aspects of planning an efficient MN's design (encompassing possible types and required properties), as well as the choice of materials and manufacturing techniques for 3D printing polymeric MNs. Next, we examine the relationship between printing techniques, the manufactured MNs, and their integration with sensors, followed by examples of studies that explore this connection. Key innovations include the use of biodegradable resins, nanocomposites, artificial intelligence, and machine learning for design optimization. While biomedical applications dominate, we highlight significant opportunities for MNs in agriculture and environmental monitoring through tailored manufacturing approaches.

1. Introduction and contextualization

The production of microneedles (MNs) and microneedle arrays (MNAs) by 3D-printing is an innovative area that directs additive manufacturing technology toward diverse cutting-edge applications. Initially focused on the biomedical field, including aesthetic treatments [1,2] vaccines [3] and diagnostics [4,5], MN-based systems are valued for their ability to analyze compounds minimally invasively compared to traditional needle systems. So far, MN sensors have been produced using various manufacturing techniques, including injection molding, machining, and advanced lithography, among others. 3D printing offers a compelling solution for prototyping and manufacturing miniaturized devices, particularly those that need parametric design optimization or benefit from mass customization [1].

The concept of MNs dates back to the 1970s, with the patent registration of a percutaneously administering drug delivery device. Specifically, the system was an array of projections ranging from 5 to 100 μm that were used to penetrate the stratum corneum and achieve pharmacological effects [6,7]. In 1995, microneedling techniques were introduced in aesthetic procedures to treat acne scars and promote collagen induction [8]. Since then, the modernization of MNs and related devices has been notable, finding use for transdermal drug delivery [9], vaccines [10], capture of fluids for clinical analysis and diagnostics [11] as well as in veterinary [12] and botanical [13] applications. Although commercially available MNs are primarily made of metallic materials, the tendency nowadays is to use polymers as major constituents, mainly using additive manufacturing, also known as 3D printing [14,15]. The relevant literature demonstrates that, for an efficient adaptation of conventional minimally invasive systems to polymer printed models, several challenges must be overcome, which involve costs, recyclability and biocompatibility of resins, and also adjustments towards scalability and production in mass [15,16]. Nevertheless, in 2020, the World Economic

* Corresponding author.
** Corresponding author. Nanotechnology National Laboratory for Agriculture (LNNA), Embrapa Instrumentação, São Carlos 13560-970, SP, Brazil.
E-mail addresses: kbr.teodoro@gmail.com (K.B.R. Teodoro), daniel.correa@embrapa.br (D.S. Correa).

https://doi.org/10.1016/j.asems.2025.100139
Received 11 December 2024; Received in revised form 30 January 2025; Accepted 10 February 2025
Available online 27 February 2025

Forum and Scientific American recognized MN technology as one of the most promising emerging technologies capable of transforming the future of healthcare [7,17]. The current knowledge and new developments in MNs indicate that there are opportunities to explore MNs' potential beyond the medical field. A survey in the Web of Science database using the keyword "microneedle" revealed a rising interest in this theme for the scientific community (Fig. 1A$_1$). Narrowing the search with terms "sensors" and "3D-printing" (Fig. 1A$_2$), it is observed the increase in the number of studies about 3D printing for MN, surpassing those that apply MN for sensors, indicating the diverse and emerging interest in 3D printed MN.

Techniques such as fused deposition modeling (FDM), liquid crystal displays (LCD), digital light processing (DLP), stereolithography (SLA), continuous liquid interface production (CLIP), and two-photon polymerization (TPP), can be performed with instruments like the schematically illustrated in Fig. 1B. These are suitable for MN and MNAs fabrication with high resolution in a fast and low-cost manner compared to conventional techniques such as molding, micro-milling, lithography, photolithography, and laser cutting. These techniques allow the fabrication of MN with different morphologies, which can be classified as solid, coated, hollow, dissolvable and hydrogel MN, as illustrated in Fig. 1C.

Biofluids like sweat, skin interstitial fluid (ISF), blood, and vegetal sap are reservoir of compounds called biomarkers, such as genetic markers of cancer [18], cholesterol [19,20], pharmaceutical products [20], and phytohormones [21]. The specific identification and the monitoring of biomarkers levels can assist the maintenance of organism homeostasis, tracking diseases or organ functions [7,22]. Interestingly, in light of global climate change, the tests of biomarkers using sensors and wearable technologies have recently been adapted from healthcare field to detect environmental stressors [22,23]. In this scenario, portable electronic devices designated to personalized Point-of-Care (POC) represent a current technology that enables the strategic planning of actions to mitigate

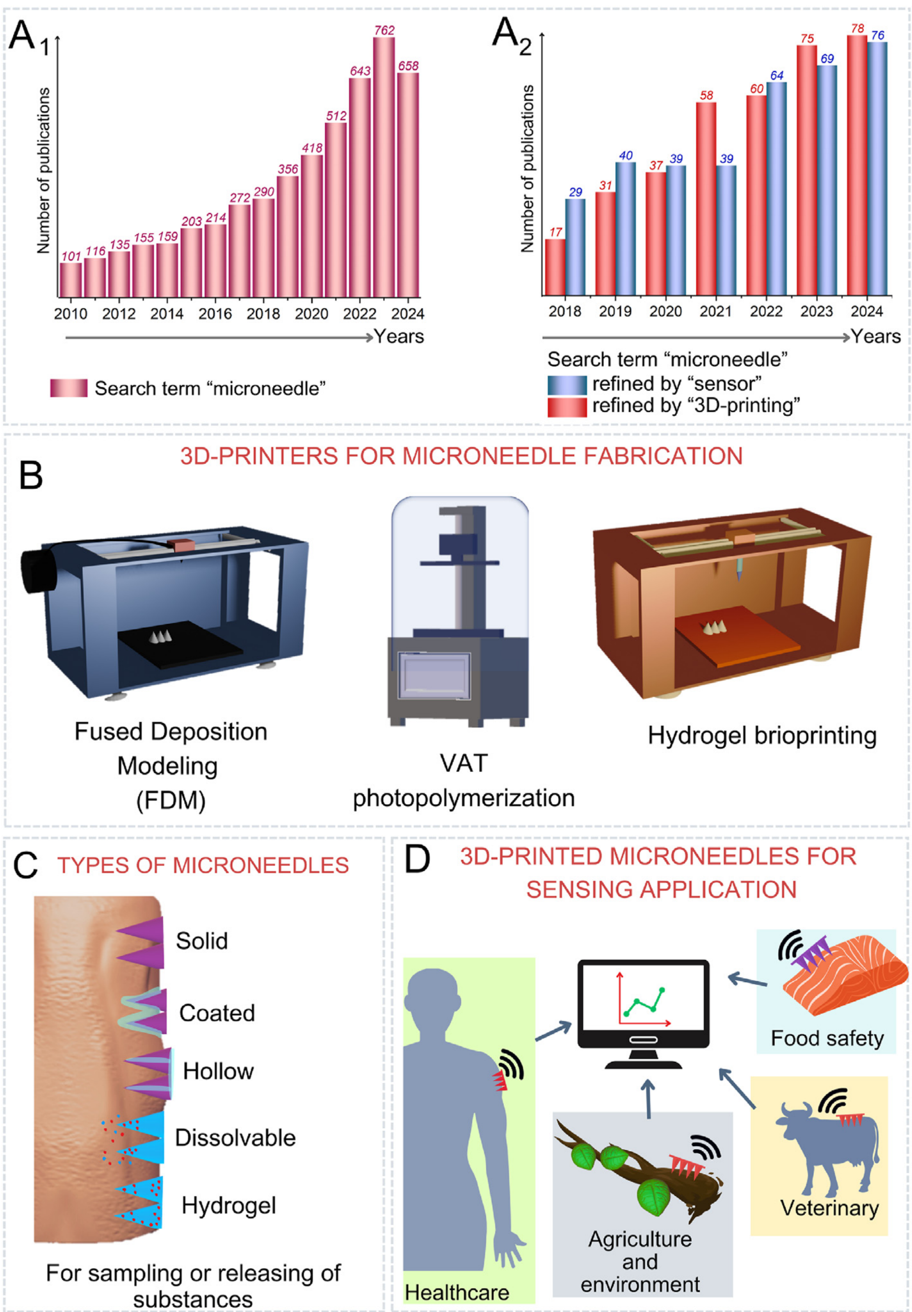

Fig. 1. (A) Graphical representation of the survey performed in the Web of Science database about the number of research articles related to (A$_1$) the keyword "microneedle", and (A$_2$) a narrower search combining the terms "sensors" and "3D printing". (B) Schematic representation of some of the instruments (3D-printers) used for MN fabrication, such as fused deposition modeling (FDM), digital light processing (DLP), and bioprinter. (C) Schematic representation of the main type of MNs. (D) Illustration of the wide variety of possible applications that can be benefited by integration of 3D-printed MNs in (bio)sensors.

issues related to healthcare [24–26], environment [27–29], food industry [30–33], agriculture [34–36], and livestock [37]. POC allows procedures and methods to be customized on a case-by-case basis, increasing the chances of effectiveness in treatments, as well as reducing inputs, and consequently, decreasing costs, wastes, and the generation of emerging contaminants. While conventional analytic methods depended on expensive and complex laboratory equipment, which makes on-site and real-time monitoring impractical, efforts to develop POC systems sparked significant interest, stimulating the development of miniaturized devices, simplified procedures, and faster analysis [38]. MNs and MNAs have generated significant interest as tools for POC tests. Consisting of miniaturized needles, with lengths of 100–1500 μm, MNs can be strategically arranged as patches [39,40], pen-shaped instruments [41,42], rollers [43,44], stamps [45,46], and syringes [47], which can pierce, with minimal invasiveness, biological tissues and other substrates [7,8]. In this scenario, they represent an attractive approach for the development of wearable (bio)sensors for continuous monitoring of relevant targets [11,33,34,48,49].

In this context, this review critically evaluates the progress in MN-based wearable sensors, highlighting their potential applications in real-time continuous monitoring of health conditions, diseases, veterinary care, plant health, and environmental sensing. Research findings published in the last 5 years (but not restricted to) were evaluated, and strategies that relate MNs application to the most suitable 3D design type, composition, and manufacturing technique are spotlighted. Despite the field of MN-based wearable sensors being currently consolidated in the biomedical and pharmaceutical sectors for health monitoring, this review discusses the most recent breakthroughs and potential applications for environmental and agricultural challenges.

2. General aspects of MNs design and fabrication

2.1. Classifications of MNs

The type, design, manufacturing technique, and composition of MNs vary according to the desired application, such as exemplified in Fig. 1D, about sensors towards different fields. MNs must be designed to effectively penetrate the tissue's protective layer in order to reach the target. In this way, MNs create micropores that facilitate the detection of substances or drug transport [50]. For instance, in health monitoring and drug delivery applications, MNs need to pierce the epidermis, reaching the upper dermal layer without reaching deeper regions containing blood vessels and nerves, thereby minimizing pain and bleeding. The ideal dimensions of MNs for this purpose range from 50 to 250 μm in width, 15–1500 μm in length, and 1–25 μm in thickness [49].

It is observed that, for sensing applications, MNs require specific sensor integration strategies, which may include a) printing of MNs and, in most cases, connected to a flexible substrate; b) integration of MN with sensing materials or electrodes; c) modification of MNs with recognition elements. Thus, the objective of integrating MNs to sensors is to combine biomolecular analysis within a single device, optimizing detection technologies. These systems can be classified as mass, magnetic, electrochemical, and optical, depending on the transduction principle employed for the detection [50,51]. The MNs associated with sensing devices can be classified into five main categories [52,53]: 1) solid MNs; 2) hollow MNs; 3) dissolvable MNs; 4) coated MNs; and 5) hydrogel-forming MNs, as illustrated in Fig. 1C and also depicted in SEM images shown in Fig. 2A–E.

2.1.1. Solid MNs

Solid MNs are fully filled structures and can be fabricated using ceramic materials, nickel, stainless steel, titanium, silicone and polymer resins [59]. From solid MNs, the transport of substances, whether for sensing or delivery applications, occurs via passive diffusion [49,52]. For biomedical applications, solid MNs create microchannels upon insertion into the skin's superficial layer, facilitating the transport of bioactive compounds to deeper layers. In comparison to intramuscular administration, solid MNs demonstrate advantage in vaccine delivery, for instance, providing a longer duration of action [60]. In agricultural applications, MNs are utilized to administer agrochemicals into plant tissues. The microchannels created by the needle insertion temporarily increase tissue exposure to agrochemicals, promoting greater absorption [61].

In sensing applications, solid MNs can be modified in order to create electrode materials for electrical or electrochemical purposes. Approaches involving the coating of solid MN with conductive materials are commonly found in literature [62], and will be discussed in the next section. Solid MNs are considered easy to prepare, cost-effective, and, in certain cases, reusable [52]. The choice of materials plays a crucial role in determining mechanical strength, biocompatibility, and reuse capability. However, for agricultural applications, repeated interventions in the field may present operational challenges. To address this issue, an increase in MNs density has been proposed, allowing for larger quantities of agrochemicals per application, thereby reducing the frequency of interventions [61].

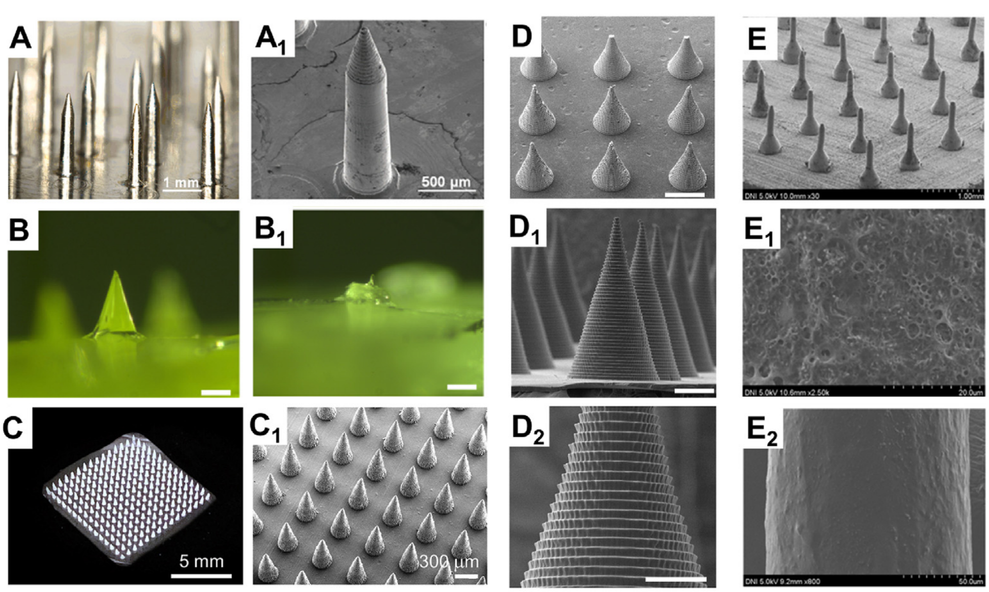

Fig. 2. Distinct types of MNs that can be employed in sensing devices. (A and A_1) Optical and SEM image of solid MN. Reprinted with permission from Cheng et al. [54] Copyright 2022, Elsevier. (B and B_1) Freshly produced dissolvable MN, and MN after 15 min of dissolution. Reprinted with permission from Tian et al. [55] Copyright 2022, Elsevier. (C and C_1) Photograph and SEM image of hollow MN patch. Reprinted with permission from Paul et al. [56] Copyright 2019, American Chemical Society. (D, D_1 and D_2) SEM images of hydrogel MN patch, tilted view (30°, scale bar: 500 μm) and Front view (scale bar: 200 μm), respectively. Reprinted with permission from Yi et al. [57] Copyright 2023, American Chemical Society. (E, E_1 and E_2) SEM image of MN array, porous coated MN containing therapeutics in the pores prior to coating of the Eudragit S100 film and after coating the Eudragit S100 film, respectively. Reprinted with permission from Ullah et al. [58] Copyright 2021, Elsevier.

2.1.2. Coated MNs

Coated MNs are solid structures whose surface was modified with materials or bioactive compounds, such as conductive materials, nanoparticles, macromolecules, elements of recognition, drugs, etc. In the context of biomedical applications, these MNs must pierce the skin and release or collect substances [52]. Besides, for efficient drug delivery, the amount of compound delivered directly depends on the geometry and size of the MNs, which affect the coating thickness and reliability of the coating process [60]. For instance, Ullah et al. [58] developed MNs capable of breaking biofilm barriers and releasing drugs in a pH-responsive manner within wounds. Metallic MNs were coated with a porous layer of poly(lactide-co-glycolide) (PLGA) designed for drug loading, where the PLGA was coated with a gelatin layer, which not only imparted porosity to the structure but also aided the healing process. This layer was then coated with an Eudragit S100 film, a pH-sensitive polymer. Eudragit S100 is insoluble in acidic pH, maintaining the film's integrity in healthy environments and preventing premature drug release. However, in alkaline pH conditions typical of wounds, Eudragit S100 dissolves, delivering the drug directly to the affected site [58]. This type of strategy can also be applied to polymer MNs. For instance, modifying MNs by attaching components responsive to the analyte of interest on the MNs surface [63] was a strategy adopted by Sulaiman et al. [64]. The authors reported the use of poly(L-lactide) (PLLA) MNs coated with alginate and peptide nucleic acid (PNA) for the isolation and detection of nucleic acid biomarkers within skin interstitial fluid. The attached PNA can be modified to match the complementary miRNA of interest. In the study, the authors used a PNA complementary to a biomarker associated with early systemic melanoma recurrence, enabling minimally invasive monitoring. In addition to being minimally invasive, the use of hydrogel MNs offers the advantage of collecting a larger volume of interstitial fluid over a short period due to their swelling capacity.

2.1.3. Dissolving MNs

In contrast to solid MNs, which are typically fabricated from metallic or ceramic materials, soluble MNs are predominantly developed using natural, water-soluble, inert, biodegradable, and bioresorbable polymers. These MNs have gained attention due to their low waste generation, as they gradually dissolve upon insertion into the skin, releasing the drug in a controlled manner within the body without the need for subsequent removal [52]. Among their main advantages are high drug-loading capacity, simplified manufacturing processes, and ease of application. Due to their dissolution characteristics after insertion, these MNs are particularly suited for drug delivery rather than applications as biosensors [61]. In this context, Tian et al. [55] investigated the development of MNs containing influenza antigens. In ex vivo tests with human skin, the MNs exhibited adequate stiffness to penetrate the skin and completely dissolved within 15 min. In experiments involving vaccine inoculation in mice, using MNs, it was observed that the immune response, measured by antibody titers, was comparable to that obtained in mice vaccinated through conventional intramuscular injections.

2.1.4. Hollow MNs

Hollow MNs resemble hypodermic needles, albeit on a smaller scale, and are promising for drug delivery and sensing applications. These MNs feature an empty interior, allowing them to be filled with drugs for controlled drug delivery applications or to have their inner surface modified with receptors, making them suitable for use as sensors [52]. This type of MNs is one of the most explored for detection purposes, mainly for sampling (procedure employed to extract and concentrate analytes), resulting in improved detection limits and greater precision in sensory analyses [61]. Morphologies with microchannels, like hollow MN, are particularly explored for electrochemical configurations, since filling MN apertures with conducting materials has proven to be an effective strategy for fabricating miniaturized electrodes [20,65,66]. However, designing these MNs presents challenges, such as structural fragility and the risk of clogging. To address these issues, strategies such as using a tapered design instead of straight structures and incorporating lateral openings have been proposed [52].

2.1.5. Hydrogel-based MNs

Hydrogel-based MNs work similarly to dissolvable MNs, eliminating the need for removal after insertion in the body. However, they stand out due to their higher drug storage capacity, making them particularly suitable for controlled drug release applications [67]. Once inserted into the tissue, these MNs absorb biological fluids, which results in the swelling of the structure and the subsequent formation of channels that facilitate the controlled diffusion of the substances, either for sampling or delivery [53]. For sensing applications focused on diagnostics and monitoring, sensing elements can be incorporated into the matrix of the hydrogel. Upon interaction with the target on biofluids, responses based on the chosen detection method are collected [50].

Among the main advantages of hydrogel MNs, compared to other types of MNs, are the absence of sharp residues after use and the possibility of production from abundant and biocompatible materials [68]. Unlike solid MNs, hydrogel MNs interact more effectively with the skin, avoiding needle retraction issues that can compromise signal efficacy. Furthermore, solid MNs can trigger immune responses upon insertion into the skin and present a risk of needle breakage at the application site [69].

To develop effective and compatible new devices, Ausri et al. [69] investigated the efficiency of hydrogel MNs composed of poly(3, 4-ethylenedioxythiophene): polystyrene sulfonate (PEDOT:PSS), hyaluronic acid, and dopamine, for ketone monitoring to prevent diabetic ketoacidosis, a severe complication of type 1 diabetes. Dopamine was used for continuous and real-time measurement of ketone bodies and as a cross-linking agent, ensuring the stability of the detection components within the hydrogel. Hyaluronic acid was selected for its ability to covalently interact with dopamine, while PEDOT:PSS was incorporated to enhance electrical conductivity. The highly cross-linked MNs exhibited good mechanical strength, allowing efficient skin penetration while maintaining flexibility and tissue compatibility. Electrochemical analyses showed that the MNs were able to detect ketone levels with a sensitivity of 0.08 mM and values within a concentration range of 0.6–1.5 mM, enabling early monitoring of the onset of diabetic ketoacidosis.

Considering environmental sensing applications, Yi et al. [57] investigated the development of a hydrogel MN patch based on sodium hyaluronate and polyvinyl alcohol with Ag nanoparticles. The system was employed for the simultaneous detection of Thiram and Thiabendazole (TBZ) residues on the surface and interior of agricultural products, respectively, in an efficient and minimally invasive manner. The MNs were fabricated using molds obtained via 3D printing, providing a structure with a high surface area. The design of the hydrogel MNs allowed their efficient insertion into agricultural samples, absorbing TBZ within the interior, while the patch base detected Thiram on the surface, enabling simultaneous detection, which is difficult to achieve with conventional sensors. The results demonstrated that the hydrogel MNs exhibited sufficient mechanical strength to penetrate the samples, and that the addition of sodium hyaluronate polymer increased the MNs swelling capacity, making detection analyses faster and more efficient. Sensing studies were evaluated using surface-enhanced Raman spectroscopy (SERS) and demonstrated detection limits of 10^{-7} and 10^{-8} M for thiram and TBZ, respectively.

2.2. Criteria for MNs properties

When it comes to MNs, the desired final application is the main factor determining the essential properties that the device must possess. However, most MNs require a set of key parameters and properties during development, encompassing structural, mechanical, chemical, and functional characteristics [70–73]. The first property to consider in MNs is the mechanical strength. To ensure efficient penetration, MNs need sufficient strength and rigidity to avoid breaking or deforming during insertion into human skin or plant tissues [71,73]. Optimizing the size of

MNs is also crucial to minimize excessive tissue damage. Therefore, the MNs should display precise dimensions, including specific diameters and lengths that allow them to reach only the target layer. The properties of the needle are influenced by the material employed, geometry, and especially by the shaft width, which generally ranges from 10 to 300 μm [73]. Details regarding mechanical evaluation and geometry aspects have been explored in the literature and are presented in the next topic. The second critical property is biocompatibility [74,75]. For human applications, the materials used in MNs must reduce the likelihood of adverse reactions and avoid triggering immune rejection. A similar principle applies to applications in plants, as MN insertion may activate defense metabolite release if the plant's system perceives the device as a threat. A third essential property for MNs is chemical functionality, particularly for MNs designed to release pharmaceutical substances, nutrients, or pesticides in a controlled manner. Incorporating these substances within or on the surface of the MNs should allow controlled release for efficient absorption by human or plant systems [70,71,73]. For environmentally friendly MNs, an essential property is the biodegradability or recyclability of the materials employed [72]. This is especially important for devices used in environmental or agricultural monitoring, where MNs may remain in the environment after use. Finally, environmental and chemical stability is necessary. For outdoor applications or extended use in humans, MNs must withstand humidity, temperature variations, and UV exposure without compromising their mechanical or chemical properties [72].

2.2.1. Mechanical properties

The mechanical properties of MNs are a critical parameter and must be carefully evaluated, as MNs need to withstand significant stress to penetrate barriers such as the skin or other materials under analysis. During tissue piercing, MNs may encounter considerable resistance, making it essential for them to possess adequate mechanical strength to avoid deformation, bending, or fracture. Mechanical issues, especially with solid MNs made from metals, glass, ceramics, or silicon, can compromise the efficiency and long-term safety of the process [76]. The substrates to be pierced comprise multiple layers, like the skin stratum corneum, the main barrier against MN penetration [76]. In the case of skin, besides the mechanical properties of MNs, it is equally important to consider the mechanical characteristics of the skin, which vary depending on factors such as the patient's age and body region. Viscoelasticity, for example, is a vital characteristic, as it provides elasticity to the skin, enabling it to stretch under external forces [77].

The mechanical strength of MNs is typically evaluated by tests that include axial and lateral force application, plate resistance testing, buckling, and flexibility tests. Among these tests, axial and lateral forces are primarily assessed. Axial force is defined as a product of the yield strength of the needle matrix material and the cross-sectional area of the needle tips. Reducing the needle tip radius can, in turn, minimize the risk of MN buckling, where the buckling force is the maximum force MNs can withstand before fracturing. The axial force test involves applying a compressive force perpendicular to the MN base. During the test, force-displacement curves are obtained by moving metal plates against the MNs and recording changes in displacement and applied force. The point at which the force changes abruptly imply in the MN's breaking point [53]. Similarly, lateral force tests follow the same principle as axial tests, but involve applying transverse forces parallel to the MN base. MN fracture resistance, as in axial tests, is also measured through force-displacement curves, which are critical metrics for evaluating structural stability [53]. Moreover, for MNs to remain stable and withstand applied forces without undergoing deformation or fracture, the minimum applied force should be lower than the buckling and flexibility force. This ensures that MNs possess adequate mechanical strength for safe and efficient applications [60,76].

Stress-strain curves are widely used to assess tensile strength, elongation at break, and tensile modulus. In stress-strain curves, the material's elastic region is identified at the start of the curve, representing the elastic deformation where the applied stress is proportional to the strain. At a certain point, the material reaches a critical juncture where it undergoes plastic deformation. Increased applied stress eventually leads to material rupture, thus defining a breaking point [76]. Another essential aspect is related to the base that supports the MNs, which also needs to be sufficiently robust and flexible to adapt appropriately to the application surface. Bending tests are thus conducted to evaluate its resistance and adaptability [76,78]. However, insertion tests on real skin are crucial to validate simulated mechanical tests. Finally, it is important to note that the mechanical properties of MNs are directly influenced by several factors, including material composition and geometric parameters such as thickness, length, and needle diameter. These factors play an essential role in determining the efficacy and durability of MNs in practical applications [76].

2.2.2. Geometry

Needle geometry not only directly influences mechanical properties but also determines drug loading in biomedical applications. The most evaluated shapes in MN development include conical and pyramidal configurations [79]. In this context, Li et al. [80] explored different MN geometries for delivering the drug Ovalbumin (OVA), assessing conical, cylinder-conical, rectangular-pyramidal, and hexagonal-pyramidal needle geometries. In rat skin insertion tests, conical MNs showed superior performance, with 95% penetration efficiency, while the other geometries demonstrated lower performances. Cylinder-conical MNs, for instance, achieved an insertion efficiency of only 40%. Dissolution tests further indicated that conical MNs were also the most efficient, achieving complete dissolution within 20 min. In subsequent drug delivery tests, these conical MNs demonstrated delivery efficiency comparable to conventional hypodermic injections, establishing themselves as an effective alternative for drug administration.

2.2.3. Additional properties for sensing application

The application of MNs as electrochemical, colorimetric, and fluorescent sensors requires some key additional properties [49,81]. In the case of impedimetric and electrochemical sensors, the MNs should present electrical conductivity to ensure efficient signal transduction, optimizing reaction efficiency and accurate signal transmission [82]. This can be achieved by using conductive layers made of metals (Au or Pt) or carbon-based nanomaterials (graphene or carbon nanotubes) [83–86]. Furthermore, MNs should allow for surface functionalization, which enables the addition of specific molecules or enzymes to enhance the detection of biomarkers or target compounds, especially for optical or colorimetric sensors that provide a visual response [49]. This functionalization promotes specific interactions between the MN surface and analytes of interest, contributing to the sensitivity and selectivity required for diagnostic and environmental monitoring applications [87–90]. Finally, another crucial property of sensory MNs is electronic integration. MN-based sensors often pair with portable electronic circuits to transmit real-time data, requiring MNs to be easily integrated with electronic chips or wireless communication systems as Wi-Fi or radio frequency [15,87,91–93]. This design allows data transmission without compromising signal integrity.

2.3. Polymers and composites for MNs manufacturing

A broad range of materials and their combinations have been proposed for MNs fabrication. Biocompatible polymers are suitable alternative materials owing to their lower costs, safe disposal after use, and adaptability for more affordable techniques of fabrication [15]. However, for the effective replacement of conventional metallic MNs, the polymeric microstructures must present specific properties, including biocompatibility, low-cost, ability to pierce the skin and endure sterilization process [94,95]. The balance between performance metrics and cost requires careful consideration regarding precise planning of the geometry, in order to avoid deformation or breakage during application, as well as in experimental procedures, avoiding, for example, shrinkage during curing or degradative effects during preparation steps. In order to fabricate structures with adequate durability and mechanical strength, it can be inspired or adapted from existent investigations that demonstrate such improvements. For example, polymer MNs capable to pierce the skin without compromise their structures and, in some cases, with penetration ability superior to metallic MNs of similar geometries have been reported [96–98].

Methacrylated biopolymers have enabled the development of photopolymerizable resins used for MNs manufacturing via 3D printing [99–102]. This approach is interesting as it encompasses natural polymers, such as cellulose, chitosan, chitin, and starch, as well as its derivatives, enabling the fabrication of sustainable and eco-friendly devices [40]. Liquid photopolymerizable resins used for molding and 3D printing are composed of reactive monomers and/or oligomers containing methacrylate and epoxy groups, which can photopolymerize in the presence of a photoinitiator and exposure to light, resulting in three-dimensional polymer networks [103]. These resins are primarily petroleum-based, although recent studies have made advances in the use of biopolymers such as cellulose [104,105], hyaluronic acid [101,106], bovine serum albumin [107], chitosan [108], gelatin [102] among others. For biopolymers to be feasible as photopolymerizable resins, chemical modifications are necessary to introduce groups susceptible to radical crosslinking, as occurs with the grafting of methacrylate groups, known as methacrylation [104,109]. Hydrogels for 3D printing also involve methacrylation and photopolymerization of diverse polymers, and the use of biopolymers for this type of application is a growing tendency.

One of the most explored biopolymers for producing photopolymerizable resins with high scaling potential is cellulose, as its occurrence and abundance are directly associated with plant biomass [110,111]. Due to its natural availability and its abundant presence as a waste product in the paper industry, cellulose has been used in studies that aim at replacing fossil-derived materials for a variety of applications, ranging from packaging [112] to biomedical applications [107]. Cellulose is a linear polymer made up of repeating β-(1 $\rightarrow$ 4) glucopyranose units and can also be represented by the repeating cellobiose dimer unit, with each β-D-glucopyranose ring originally having three hydroxyl groups, including two secondary alcohols (on carbons C2 and C3) and one primary alcohol on carbon 6, which is more reactive and susceptible to substitution than the other hydroxyl groups [113,114]. For instance, from carboxymethylcellulose (CMC) and cellulose nanocrystals (CNC), Soullard et al. [104,105] reports the esterification at the hydroxyl group on the C6 carbon of the unsubstituted glucopyranose ring, resulting in methacrylic anhydride (MA) producing cellulose-based photocrosslinkable aqueous formulations. Attempts of printing objects showed that the formulations have the potential to manufacture 3D structures. Formulations using a biocompatible photoinitiator and the methacylated CNCs added as fillers, showed stable colloidal properties in water, which reduced crosslinking time and preserved hydrogel elasticity after swelling. The cryogels were cytocompatible with fibroblast cells, highlighting the potential of these formulations in medical applications.

The use of composites and nanocomposites in MN is also feasible and, while their application is still limited, it can benefit from the unique properties and significant advantages offered by nanoscale materials and devices [115,116]. The high surface area-to-volume ratio, high load capacity, and the ability to tailor the size, morphology, and surface chemical composition of nanostructures for specific applications have driven nanotechnology to contribute across various fields of knowledge, including biomedical applications, bioimaging [117,118], drug delivery [119–121], and diagnostics [122–124]. Studies exploring the combination of nanomaterials to polymer resins directed to 3D-printing fabrication of MN are still sparse. This observation indicates the space for novelties, exploring nanostructured formulations and the broad spectrum of additional properties that nanomaterials can provide.

2.4. Fabrication of polymer MN by 3D printing technologies

Additive manufacturing (AM) encompasses a set of versatile 3D printing technologies that enable the fabrication of three-dimensional structures with complex geometries through the controlled layer-by-layer deposition of varied materials (metal, ceramic, or polymer) [125–127]. The first step involves creating a model and designing the structure to be printed using CAD-based software [128–130]. Next, a Standard Triangulation Language (STL) file format is generated, which is the standard data format for this process [131]. The file is then transferred to the 3D printer, where it is sliced into layers for the construction of the designed 3D structure.

3D printing technologies enables major advances in the fabrication of custom MNs with complex geometries [132,133] with high resolution and easy application, achieving fast, low-cost, clean production with less material waste [134–136]. These aspects set this approach apart from conventional techniques (molding, micro-milling, lithography, photolithography, and laser cutting) [137–139]. Despite this, challenges still need to be overcome regarding the selection of the material to be printed, as well as the mechanical resistance, biodegradability, and biocompatibility of these devices [133,140,141]. Given this, MN manufacturing by 3D printing technologies based on FDM, and VAT photopolymerization stand out. A schematic representation of the most explored 3D-printing techniques is shown in Fig. 3.

FDM technology is based on the melting of thermoplastic polymers (in the form of filaments), followed by the extrusion and deposition of the molten material layer-by-layer on the heated printing surface, where the material solidifies, taking on the designed shape [144]. Due to the viscoelastic characteristics of polymers, thermoplasticity plays an important role in shaping the molten and extruded filament, as well as in the adhesion between the deposited layers after solidification [145,146]. Printing parameters such as extrusion nozzle diameter, processing temperatures, speed, orientation, and printing angle may also promote under-extrusion, surface defects, low quality, and loss of mechanical strength of the printed material [147–149].

FDM technology is the most popular among additive manufacturing technologies, due to its easy accessibility, low cost, fast production, non-use of solvents, and the possibility of printing flexible or rigid devices [150,151]. However, it is worth highlighting some limitations of this technology, such as the temperature gradient generated at the time of printing, biocompatibility, and low resolution of the devices [146,152]. Actually, many polymers have been processed by FDM [153], and it is worth highlighting the possibility of producing filaments incorporated with graphene, carbon nanotubes, graphite, or carbon black to improve the mechanical, electrical, and thermal properties of 3D-printed materials [154–158]. Concerning the production of MNs by FDM, the effect of 3D printing parameters on the dimensional accuracy and geometry of these devices stands out, in addition to the possibility of carrying out post-printing chemical treatments aimed at improving both the size and shape of the MNs [159,160]. The manufacture of biodegradable MNs capable of acting as platforms for transdermal drug delivery has also been reported [161].

VAT photopolymerization brings together a set of 3D printing technologies that encompasses SLA, DLP, TPP, LCD, and CLIP [153]. For this purpose, photocurable resins [162–165] based on bisphenol A diglycidyl ether (DGEBA), pentaerythritol tetraacrylate (PETA), dipropylene glycol diacrylate (DPGDA), or trimethylpropane triacrylate (TMPTA) have been used, or polymers functionalized with methacrylate groups based on gelatin [166]. Silk fibroin [167], poly(2-hydroxyethyl methacrylate) [168], carboxymethyl cellulose [169], chitosan [170] and hyaluronic acid [171,172] can also be used as substrate. Fundamentally, the 3D printing process occurs in the presence of a photoinitiator, such as: bis(2,4,6-trimethylbenzoyl) phenylphosphine oxide (Irgacure 819), bis(2,4,6-trimethylbenzoyl) phenylphosphine oxide, diphenyl(2,4,6-trimethylbenzoyl)phosphine oxide (TPO), 2,2′-azobis-2-methyl-N-(2-hydroxyethyl)propionamide oxide (VA-086), 2-hydroxy-4′-(2-hydroxyethoxy)-2-methylpropiophenone (Irgacure 2959) and 2,2,6,6-tetramethyl 1-pyridinyloxy (TEMPO)

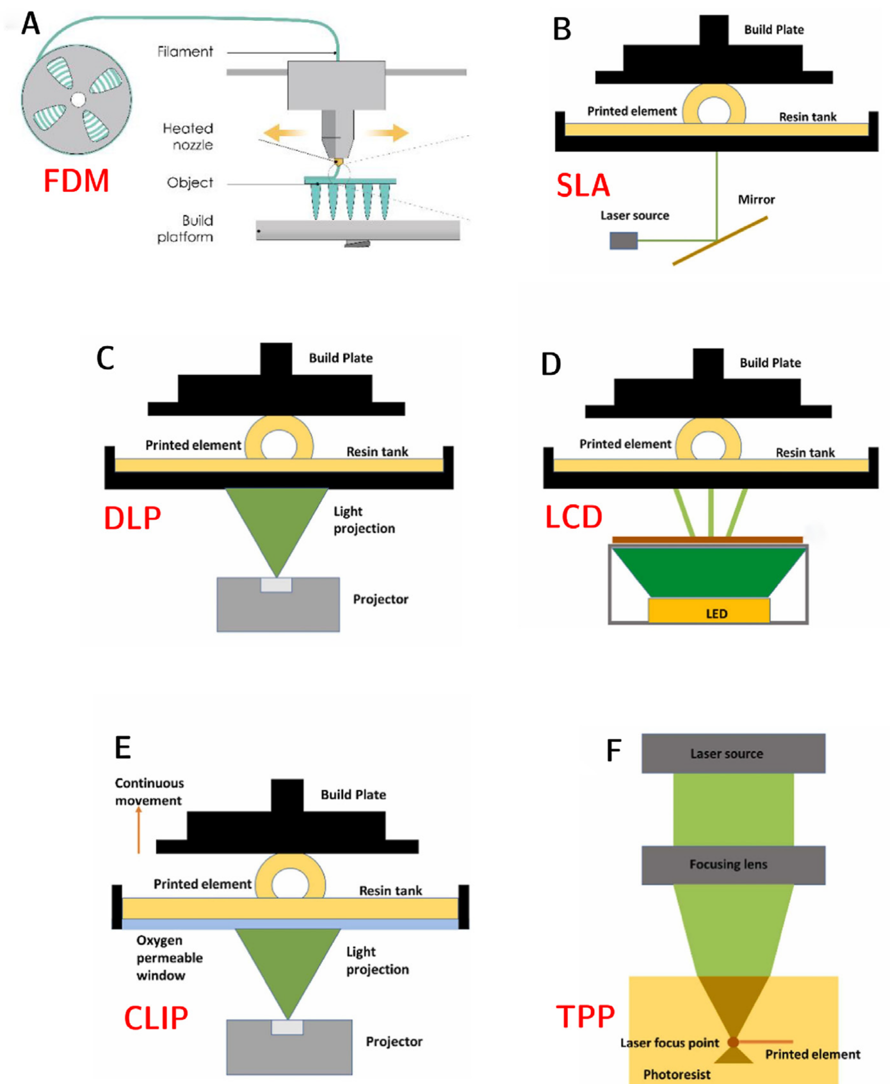

Fig. 3. Schematic representation of different 3D printing technologies. The main elements of the instruments used for each technology are indicated. The abbreviations located at left side of each scheme are related to the name of the technique, as follows: (A) FDM, (B) Stereolithography, (C) DLP, LCD, CLIP, and TPP. Figure adapted from Sirbubalo et al. [142] Copyright 2021, MDPI, and Chekkaramkodi et al. [143], Copyright 2024, Elsevier.

[173–176]. The polymer solutions containing the photoinitiators are placed in a tank and then exposed to ultraviolet (UV) radiation in the range of $\lambda = 365$–405 nm [177–179]. It is worth noting that each technology based on photopolymerization in a vat will present its intrinsic issues concerning speed, time printing capacity, resolution, and precision of the devices constructed [180–182].

In the search for better processing conditions for materials in photopolymerization using VAT, composite materials have been developed that allow obtaining customized high-resolution products, with better mechanical resistance properties (tensile or compression), high corrosion resistance, and low cost [183] since using only one material it is difficult to meet all project demands [184–187]. Thus, by combining the materials, composites have been developed that are capable of meeting piezoelectric demands, through the incorporation of barium titanate [188] filtration through the addition of alumina microparticles [189], improvement of mechanical resistance through the creation of new photopolymerizable resins based on methacrylate and acrylate extracted from green sources [190], increase of electrical conductivity through the combination of the polymers poly(3,4-ethylenedioxythiophene): polystyrene sulfonate (PSS) and polyethylene glycol diacrylate (PEGDA) in aqueous solution [191] increase in the sintering temperature through the incorporation of aluminum nitride and yttrium oxide to the photosensitive resin [192].

LCD and CLIP technologies stand out in the fabrication of MNs by in-VAT polymerization. In LCD technology, devices are built bottom-up [193]. Besides, LCD is used to manufacture hollow devices with complex geometries, at low cost and with a vertical resolution of ~50 μm and a horizontal resolution of ~150 μm [194]. From the literature review, only a few works have demonstrated the fabrication of devices based on MNs by LCD for the sensor area. Alternatively, the published works are focused on the controlled release of drugs [195–198]. CLIP technology [3] uses an oxygen-impermeable window that inhibits photopolymerization, preventing the adherence of the constructed part to the printing window [199]. Thus, the polymeric material can flow freely into the so-called “dead zone” [200], allowing continuous layer-by-layer production [201,202], making it possible to produce high-resolution devices [203], such as square-based pyramidal geometry and designs, using polymers such as trimethylolpropane triacrylate, polyacrylic acid, and photopolymerizable derivatives of polyethylene glycol and polycaprolactone, in fast production times (<10 min) [204]. Similarly to LCD, MN-based devices manufactured by CLIP technology are focused on the drug delivery [3,205]. It is worth noting that LCD and CLIP technologies have not yet been employed to fabricate MN-based platforms to act as sensors, suggesting opportunities for new research efforts.

Regarding the fabrication of MNs and MNAs for sensing applications, the most explored technologies are based on SLA, DLP, and TPP. Thus, SLA technology has enabled the development of devices used in the controlled release of high molecular weight antibiotics [206] treatment of human squamous cell carcinoma A431 [207], as well as to detect diseases in plants caused by bacteria [208]. Using SLA technology, it is possible to fabricate solid MNs smaller than 100 μm [142]. Moreover, the curing times of the deposited layers range from 2 to 100 s, resulting in printing speeds ranging from 5 to 1000 mm/height, and layer heights range from 25 to 200 μm, allowing structures with resolutions of up to 100 nm to be obtained [209,210]. SLA also allows the construction of 3D structures using the free surface method, where parts are manufactured from the bottom up from a support platform that rests just below the resin surface, or using the constrained surface method where a construction platform can be suspended above the resin bath [142,211].

Another AM technology used in the production of MNs is DLP, which enables faster manufacturing due to the greater exposure of the polymer solution to UV radiation in a smaller area [180]. In this case, DLP employs a digital light projector, in contrast to SLA technology, which is point-based and relies on mirrors to direct the light [212]. Besides, DLP technology has a pixel printing method that allows for the construction of small devices with complex geometries displaying high resolution and precision [213]. DLP technology has enabled significant advances in the manufacture of customized MNs concerning printing parameters [214], type of polymers [166,215,216] and photocrosslinkers [175], crosslinking time [217], device design [218], mechanical properties [217], controlled drug delivery [2,219–222] and biocompatibility [223].

TPP is another 3D printing technology employed in the fabrication of MNs [224–226]. It uses focused ultrashort laser pulses to promote the phenomenon known as "two-photon polymerization" in a well-localized spatial region of the sample. This technique can be used for photosensitive resins, hydrogels, and composites [227–230], enabling the fabrication of complex layer-by-layer structures at the micro- and nanoscale [231,232]. By using TPP it is possible to produce MNs with a high degree of control over the designed geometry [14,227,233,234], also allowing to obtain MNs in different geometries for controlled drug release. For instance, MN can be obtained using TPP with a variety of dimensions and shapes. These include heights ranging from 200 to 400 μm, inner diameter of 80–120 μm, tip wall thickness of 5 μm [75], height of 900–1300 μm, in conical, pyramidal, cross-shaped and pedestal shapes, with base widths of 300–500 μm and spacing 100–500 μm [235]; and conical devices with 3 × 3, featuring heights of 800 μm, base diameter of 250 μm, needle diameter of 30 μm, inter-needle distance of 1000 μm, and base height of 50 μm [236]. While TPP enables the fabrication of MN with high resolution, on small scales, it presents some drawbacks. These included materials shrinkage after photopolymerization, which can result in structural defects in the final product [237], the low biocompatibility of commonly used resins, lengthy processing times, high production cost, the need for photosensitive materials and challenging in maintaining the integrity of the printed devices [138].

In comparison to traditional micromolding methods, 3D printing has been shown to be more suitable for MN manufacturing, offering enhanced precision, customization, and scalability. This technology enables the fabrication of MNs with the high dimensional accuracy necessary for precise applications, leading to improved performance and expanding their potential uses. However, challenges remain, particularly regarding scalability and regulatory compliance, which must be addressed to bring 3D-printed MNs closer to commercialization [238,239]. As the adoption of 3D printing in MN fabrication is relatively recent, establishing efficient large-scale production processes will require time and refinement. Manufacturers must evaluate the cost efficiency of 3D printing compared to traditional techniques, particularly for mass production [238,240]. Additionally, advancements in printing technologies are crucial to address the trade-off between print resolution and build size, ensuring scalable and consistent production [239]. The different 3D printing methods offer unique advantages based on resolution, material compatibility, and also scalability. Techniques like SLA and DLP, for instance, deliver high-resolution capabilities, making them ideal for intricate MN designs, while FDM provides cost-effective scalability and versatility in material selection, suited for larger-scale production [239,240]. Conversely, TPP, while capable of producing highly detailed structures of small dimensions, faces challenges related to high costs and lengthy production times, limiting its scalability [240].

3. Relation 3D-printing – microneedles – sensors

The integration of 3D-printed MNs into sensor and biosensor devices necessitates enhanced collaboration across materials science, chemistry, physics, biology, and computer science. Besides, the integration of artificial intelligence (AI) tools enables enhanced quality control by monitoring and predicting potential imperfections in the printed device shapes. AI can also assist in selecting materials for specific 3D printing technologies, optimizing drug selection for disease treatments, and intelligent monitoring of various biomarkers, such as glucose, urea, acetylcholine, alcohol, and glutamate, in real time. To achieve this, it is essential to integrate these sensing platforms to IoT technology [241–244]. Moreover, practical issues associated to the long-term use of MNA as sensors, as well as for real-time analysis, face technological challenges and need to be evaluated in a multidisciplinary way. It includes fixing on the surfaces, stability of the electrochemical signals during monitoring, data reliability and biofouling. Some technological barriers in sensor integration within MNs can be overcome with previous planning. Achieving high sensitivity while maintaining miniaturization is one of the key challenges. The small surface area of MNs can limit the space available for functionalization with recognition elements (e.g., enzymes, aptamers, or antibodies), which are crucial for selective analyte detection [245]. Moreover, due to the small sample volumes collected by MNs, the signals generated can be weak and prone to noise and interferences [246,247].

Table 1 presents a collection of information regarding the use of 3D-printed MNs for (bio)sensing, extracted from representative research articles. The literature reports that the integration of MNs in (bio)sensors devices is motivated by the more effective sampling and biomarkers capture, association with microfluidic devices, among other reasons. The strategies adopted to integrate MNs with wearable sensors are discussed and exemplified in the next topics.

3.1. MNs for sampling and biomarkers' capture

Since one of the challenges associated with ISF analysis regards to the efficient extraction of target analytes (sampling) [252], the integration of MNs into wearable sensors aims to concentrate and capture biomarkers, promoting the sampling and testing [66,252,251]. Hollow MN morphologies [252,248,258] are the primary designs explored to address sampling challenges. However, increasing interest has also been observed in solid [39], swellable [90,259,260], porous [261,262], and other [263,264] MNs shapes. Swellable and porous MN fabrications are still mainly related to techniques of molding, suggesting opportunities towards 3D printing techniques [66,252]. Investigations about strategies for sampling and detection are the focus of recent researches [66,252,254]. For instance, Cheng et al. [252] proposed a strategy to address sampling difficulties for ISF analysis, where they developed a platform that combines controllable hollow MNs and microfluidic paper-based analytical devices. The MN were fabricated using micro-SLA printing, along with a rectangular platform containing two branched channels and two circular detection areas. This platform was integrated with a bottom PDMS layer designed to produce negative pressure for sampling. Fig. 4A_1 shows the image obtained by scanning electron microscopy (SEM) of a conical MN, which contains a single channel. To guarantee the good hydrophilicity to facilitate the liquid absorption and transport, the authors applied plasma surface treatment to the MNA. The fluid draining ability was tested using a red dye solution, for better visualization (Fig.

Table 1
Examples of recent MN-based wearable sensors, detailing the MN morphologies, 3D-printing method employed for the device construction, and the sensing experiment information.

MN morphology	Sensing method	3D printing technique	Biomarker/analite	Biofluid	Ref.
Hollow	Electrochemical	DLP	Ketone bodies	ISF	[5]
	Electrochemical	DLP	Glucose, uric acid and pH	ISF	[248]
	Electrochemical	SLA	Irinotecan and SN-38 (chemotherapeutic prodrug and its metabolite)	ISF	[249]
	Electrochemical	SLA	Apomorphine	ISF	[86]
	Electrochemical	SLA	pH	ISF	[250]
	Electrochemical	LDW	Myoglobin and troponin	ISF	[251]
	Colorimetric	SLA	Glucose and lactic acid	ISF	[252]
	Colorimetric	SLA	Sodium ions and uric acid	ISF	[253]
	Colorimetric	SLA	pH	Wound fluids	[39]
	Electrochemical and colorimetric	Photocurable Resin printing	Glucose, uric acid and pH	ISF	[254]
	Strain and colorimetric	DLP	Body movement and glucose	ISF	[255]
Solid	Electrochemical	DLP	Glucose	Plasma and ISF	[256]
	Electrochemical	SLA	Buprenorphine	Intestinal fluid	[39]
Solid swellable	Colorimetric	DLP	Glucose and pH	ISF	[257]

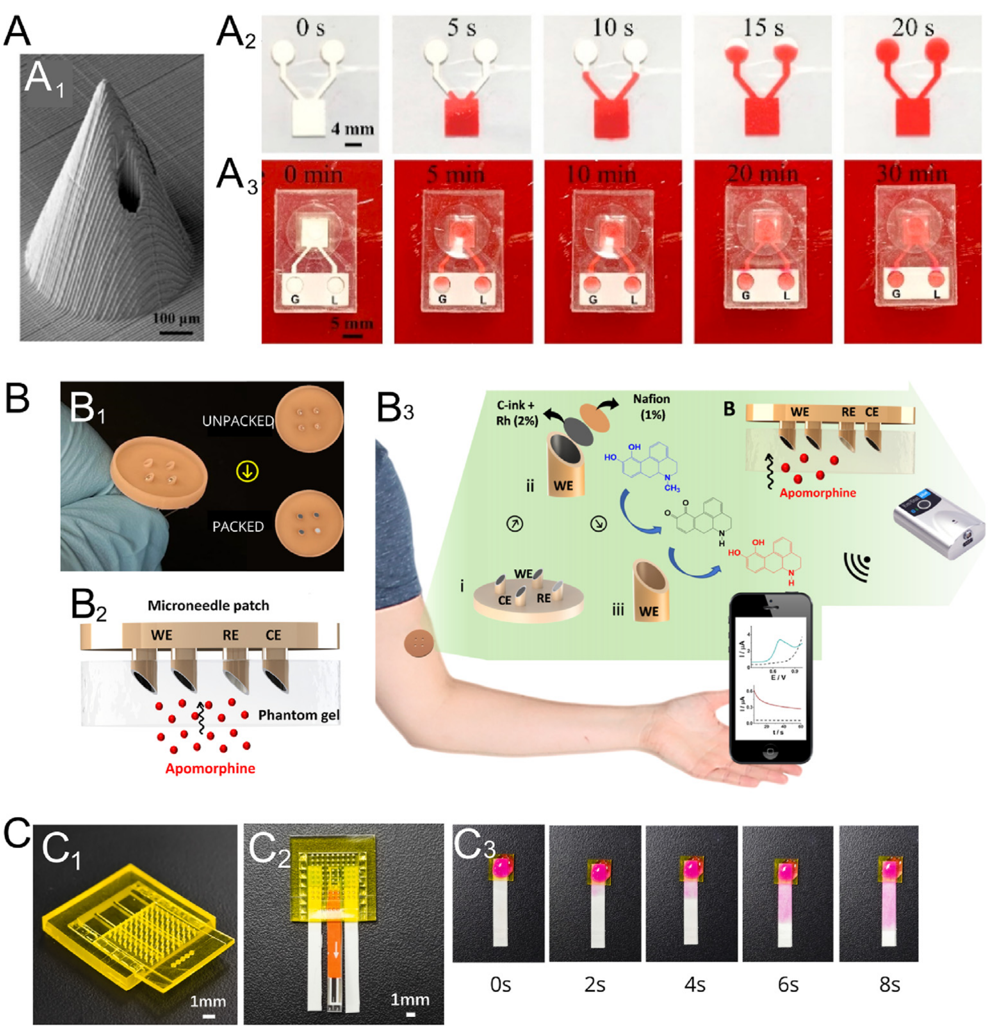

Fig. 4. Examples of approaches to integrate 3D-printed MNs in sensor and biosensor devices. (A) Design strategy used for the fabrication of a platform that combines controllable (A_1) hollow MNs and microfluidic device. A red dye solution evinces the sampling in (A_2–A_3). (A_2) shows that the liquid filled all the spaces in 20 s, including the detection area, and (A_3) shows the performance of sampling using agarose gel model, with an efficient liquid drainage after 20 min. Reprinted with permission from Cheng et al. [252] Copyright 2023, Elsevier. (B) Use of MNs as miniaturizes electrodes for electrochemical approaches. (B_1) digital images of 3D printed MNA patches (packed and unpacked), (B_2) schematic illustration of the packing of MN channels with the pastes for electrode fabrication, as well as its use in a human arm, and (B_3) the representation of the MNA with WE, RE, and CE electrode system in phantom gel mimicked skin experiment. Reprinted with permission from Goud et al. [86] Copyright 2022, Elsevier. (C) Example of MN platform for monitoring multiple biomolecules using a combination of transduction methods. (C_1) mountable structure composed of MNA patches, with compartments designed for the insertion of electrochemically and colorimetric responsive platforms, (C_2) different optically and electrochemically responsive strips to support the simultaneous detection of glucose, uric acid, and pH, and (C_3) ability of extracting fluids for further sensing, revealing capability of extract about 16 mg of liquid within 10 s. Reprinted with permission from Ma et al. [254] Copyright 2024, Elsevier.

4A_2), and the liquid filled all the spaces in 20 s, including the detection area. Fig. 4A_3 shows the performance of sampling using agarose gel model. The efficient liquid drainage ability was verified after 20 min, while the red liquid was sucked up and filled the whole spaces in response to the one-touch finger operation negative pressure. The tests conducted to simultaneous detection of glucose and lactic acid demonstrated that the system could effectively drain the fluids towards the detection sites via capillary force, by one one-touch-activation.

3.2. MNs as microelectrodes for electroanalytic analysis

Table 1 highlights that 3D-printed hollow MN have attracted significant interest for the integration with sensor devices, supporting both electrochemical [20,65,66] and colorimetric detection approaches [5,86,252,249,265]. Towards electrochemical sensors, morphologies with microchannels, like hollow MNs, can be filled with conducting materials, fabricating miniaturized electrodes [20,65,66]. Conductive pastes can be used for this strategy, as those based on graphite [266,267], and carbon composites [268–271]. Nafion polymer has been used to avoid biofouling, an issue associated with long-term measurements, beside the common purpose of contributing with the diffusion-limited layer [20,272].

Fig. 4B shows photographs and the schematic illustration of the MN array with working electrode (WE), counter electrode (RE), and counter electrode (CE) system proposed by Goud et al. [86], to be applied as a wearable sensor for apomorphine, a drug used for Parkinson disease treatment. Fig. 4B_1 depicts digital images of 3D printed MNA patches, with inter-needle spacing of 10 mm and an internal MN diameter of 500 μm. One of the images shows the unpacked hollow MNs, while the next image shows the packed MNs, adapted to act as electrodes. For this purpose, two of the four MNs were filled with rhodium-modified carbon paste and transformed in WE, while the third MNs was filled with conventional carbon paste and served as CE, and the fourth MNs was embedded with Ag wire to be used as RE. The illustrations in Fig. 4B_2 highlights the packing of the MN channels with the pastes and the disposition of the electrodes in the patch. Fig. 4B_3 illustrates the operation scheme of the MNA interacting with apomorphine in the skin mimicking phantom gel, the catalytic oxidations of catechol and tertiary amine moieties of this analyte, and the wireless data transmission to the smart device.

Research involving vivo tests has revealed practical challenges, such as the displacement of MNA after application to the skin, as noted by Reynoso et al. [273]. In response to skin contraction and movement after placing MNs in rodents, the authors observed a loss of stability in electrochemical signals, attributed to the retraction of circuits away from the skin. To improve the stable attachment of MNA-based circuits, the authors reported the integration of magnetic components into the MNA, which assisted in fixation and prevented electrode disconnection from the analysis medium. For this, a small skin incision was necessary for subcutaneous implant of flat metallic discs. By evaluating the variations in the redox signal of methylene blue, compared with medical tapes and glues used for fixing the MNA, it was observed that the magnetic fixation system of the circuits led to a stable measurement signal baseline, and more robust retention of square wave voltammetry signals over the entire measurement time.

3.3. MNs combined with microfluidic devices and multiple analysis

Also taking advantage of hollow MNs for electrochemical transduction, Wu et al. [249] an aptamer-based sensors (E-AB) using MNA designed for continuous monitoring of the chemotherapeutic prodrug irinotecan and SN-38 (its metabolite). For this, hollow dual channels were printed using poly(methyl methacrylate) resins and coated with gold by sputtering technique, over which aptamers were immobilized. The MNs were integrated into a 3D printed fluidic device designed to mimic *in vivo* excretion kinetics, demonstrating real-time drug monitoring with MN E-AB arrays. The ability to monitor the prodrug and its metabolite, simultaneously, at adjacent MNs, demonstrated the possibility of developing multiplex systems using MNs.

Advancements in MN-based sensors have enabled the transition from laboratory-based analyte detection to wearable sensors. Additionally, these developments have facilitated the combination of various transduction methods, as demonstrated in the studies by Ma et al. [254]. The authors developed a detachable MN platform capable of monitoring multiple biomolecules using a combination of colorimetric and electrochemical sensors. This platform features a mountable structure that accommodates MNA patches (Fig. 4C_1), along with compartments designed for the insertion of electrochemically and colorimetric responsive platforms (Fig. 4C_2). The insertable cavities enhance versatility, allowing customization with different test strips to support the simultaneous detection of glucose, uric acid, and pH. The platform provided a visual readout through colorimetry while ensuring high accuracy via electrochemistry, making it ideal for POC testing. For the simultaneous analysis of three classical biomarkers (glucose, uric acid, and pH), three-compartment structures were fabricated for analysis in interstitial fluid (ISF) sampled by the MNA. The ability to extract fluids for further sensing was tested, as illustrated by Fig. 4C_3, and revealed the capability of extracting about 16 mg of liquid within 10 s. The sensing studies demonstrated consistent readings that accurately reflected the concentration of the analytes within the skin models, achieving accurate measurements and ensuring their functionality and stability in rapid clinical detection.

3.4. MN for easy-to-interpret colorimetric analysis

It is expressive of the number of recent papers exploring 3D-printed MN for colorimetric sensor devices. Colorimetric platforms are interesting for POC diagnosis because they do not require the integration of complex circuits and batteries. On the contrary, they explore mechanisms that can be interpreted by human eye or by colorimetric applications (using software or devices) thereby minimizing subjective interpretations. In this direction, Xie et al. [253] reported a wearable MNA-based colorimetric sensor to monitor sodium ion and uric acid levels in elderly patients suffering from nocturia. The proposed device is composed of a MNA (bi-channel hollow), connected hoses and injection needle, a sensing unit paper, a vacuum tube able to exert adequate negative pressure to extract ISF, and a silicone wearable belt integrated with a watch. It was possible to collect approximately 14 μL of ISF within 5 min, aiming for convenience in daily use. To tackle issues of ambient light affecting colorimetric analysis, a custom model was designed to improve accuracy in varying conditions, allowing effective classification of sodium and uric acid concentrations. The sensor was tested successfully in living rat models, demonstrating potential as a point-of-care tool for use in the elderly.

In another work, Liu et al. [265] developed a multifunctional eutectogel MN (EMN) patch, which was designed for transdermal diagnostics and drug delivery, addressing challenges in the integration of MN for multiple purposes. The multifunctional EMN patches could perform multiple tasks, including monitoring body movements wirelessly, colorimetric glucose detection, and controlled drug delivery. In this case, the authors also included the use of polymerizable deep eutectic solvents (PDES) as printing inks, allowing for the fabrication of EMN patches with suitable mechanical strength and high drug solubility. Besides, the patches presented rigid hollow MN and a flexible backing layer.

4. 3D printing MNs for biomedical sensors

In healthcare scenario, personalized therapies represent the most important advances of modern medicine [274]. The use of MNs and MNAs aims [18] for a more specific tailoring and designing of medications, considering individualized physiologies, drug responses, and genetic profiles, minimizing the likelihood of ineffective dosages and side effects [18,86,274]. The Food and Drug Administration (FDA) approves the use of MN products for patients who are aged 22 years or older, and its regulatory policies for legally marketed uses, risks of using, information for patients are available in FDA digital sources [8,275]. Despite serious problems being less frequent, micro-needling can pose some risks, which are firstly associated with the piercing of skin. Although it typically heals shortly, these products may lead to discomfort, skin irritation, dryness, redness, itching, bruising, and bleeding, while more severe problems are less common [275].

In the sensors field, AM technologies are enabling the manufacture of multifunctional devices (wearable and implantable) with complex architectures and controlled microstructures. These are capable of quantifying proteins, neurotransmitters, and metabolites with greater detection range, sensitivity, lower threshold, and diagnostic capability at the point of care [276]. MN-based sensors are explored as POC products able to avoid pain due to their minimally invasiveness way to monitor biofluids, such as ISF, sweat, saliva and tears [277].

Table 1 indicates that the majority of MN-based sensors monitoring biomarkers and therapeutic drugs explores the ISF, expressing the abundance of bioinformation that this biofluid provide. For example, it enables the fabrication of MNs that can be coupled to microfluidic devices to facilitate early detection and measurement of glucose in situ in patients with type 2 diabetes [14]. They have also been used in the development of biosensors capable of monitoring in real-time various biomarkers associated with kidney disease, Parkinson's, and electrolyte disorders, as well as in the detection of cancers and diabetes [255,278]. Furthermore, important advances have been reported in the development of MNs capable of acting as electrochemical sensors coupled to electronic systems, as well as in aspects regarding the commercialization of these devices, methodology for evaluating the accuracy of these sensors, and conducting in vivo tests [11]. In another study, aptamer-decorated porous MNAs for extraction and detection of biomarkers from skin interstitial fluids were also reported [249]. *In vitro* detection results (rats) indicated that the aptamer-decorated arrays presented a highly sensitive and rapid detection of endotoxin in the concentration range from 0.0342 to 8.2082 EU/mL, with a detection limit of 0.0064 EU/mL. Another possibility reported is the manufacture of MN-based platforms capable of detecting, monitoring, and treating diseases in plants caused by fungi and bacteria, demonstrating the versatility of these devices for applications in precision agriculture [61].

With the large variety of 3D printing techniques, the resolution in the X and Y planes, as well as in the Z axis, can vary widely, ranging from a few nanometers to hundreds of micrometers [279]. FDM, for instance, stands out for its greater accessibility and simplicity, although it offers lower spatial resolution [160]. Depending on the nozzle diameter, which generally ranges from 100 to 200 μm, the fabrication of high-precision devices, such as MNs, can be hindered by these limitations [244]. To overcome these challenges, Sarabi et al. developed an innovative approach that combined PLA corrosion with KOH and artificial intelligence techniques, improving resolution and minimizing anomalies in MN manufacturing, enhancing their structural and functional features [244]. In sensor development, PLA/PVA/PVP-based MNs incorporated with the drug galantamine hydrobromide were reported for the detection of Alzheimer's disease [280]. Regarding the manufacture of MNs sensing platforms using FDM, it is important to highlight that its use is limited due to the high temperatures used to melt the filament, low printing resolution, and the slow biodegradability of PLA, a polymer widely used in the manufacture of MNs [281,282].

Although it is a simple technique with a wide range of materials that can be explored, FDM 3D-printing faces many challenges in applications involving MNs [160]. For these applications, techniques such as SLA, SLS, DLP, CLIP, and TPP provide greater suitability, as they enable achieving higher resolutions, essential for the fabrication of devices at the micro and submicron scales. Using DLP technology, Liu et al. [256] developed an integrated biosensor for glucose monitoring in diabetic patients Fig. 5A_1 and A_2, measuring glucose levels in ISF with high precision and in real-time. The study combines 3D-printing, electrodeposition, and the immobilization of the enzyme glucose oxidase (GOD). *In vitro* and *in vivo* tests, conducted on healthy and diabetic mice Fig. 5A_3, demonstrated that the biosensor reliably and accurately monitored glucose (linear detection (LD): 0.8–24 mM and detection limit (DL): 8.65 μM), showing a strong correlation with results obtained from commercial glucose monitors Fig. 5A_4, A_5 and A_6 [273]. Following this approach, Moonla et al. developed wearable MNs (WMN) based on the enzyme β-hydroxybutyrate dehydrogenase (HBD) for real-time detection of ketone bodies, such as β-hydroxybutyrate (BHB). The sensor enabled real-time monitoring through a Pt-transducer electrodeposited with Au. It was modified with an electropolymerized toluidine blue O (poly-TBO) mediator layer, followed by a biocatalytic layer containing the HBD enzyme along with the nicotinamide adenine dinucleotide (NAD^+) coenzyme. This biocatalytic layer was functionalized with carboxylated multiwalled carbon nanotubes (CNT-COOH) and Chitosan and protected by a PVC layer. The sensor exhibited linear range of 0.5–5.0 mM, with a limit of detection (LOD) of 95 μM and stability during continuous amperometric monitoring of 0.2 mM BHB over 5 h [5].

Xie et al. [283] developed a MNA patch (MAP) system for the rapid extraction and analysis of ISF. This system consisted of an array of solid, cone-shaped MNs with a base diameter of 1000 μm and a height of 1000 μm, featuring two 250 μm holes within each needle showed in Fig. 5B_1 and B_2. These MNs were fabricated with biocompatible resin through stereolithography and were connected to an ISF extraction system. The extracted fluid could be used for colorimetric analysis of various analytes and integrated with a glucometer, allowing for continuous, non-invasive monitoring [283], as shown in Fig. 5B_3.

Keirouz et al., proposed the use of MNAs coated with conductive polymers such as polypyrrole (PPy) and PEDOT:PSS. The study investigated two methodologies for coating resin MNs: *in situ* polymerization and casting. The MNs were tested on *ex vivo* porcine skin, demonstrating efficacy in penetration, mechanical durability, and electrical stability after multiple usage cycles by cyclic voltammetry. Furthermore, the coated MNs were found to be non-cytotoxic, providing a promising approach for biomedical sensors in continuous monitoring devices [285].

The TPP technique offers significantly higher resolution compared to other 3D fabrication approaches. Based on this technology, Dervisevic et al. [264] developed a WMN patch for transdermal urea monitoring in the ISF. This device uses a MNA with microcavities to protect the sending layer, preventing damage during skin insertion. The two-electrode system with a MNA coated with Nafion and layers of polyaniline and urease enabled selective urea detection, exhibiting a sensitivity of 2.5 mV/mM, a linear range of 3–18 mM, and a LOD of 0.9 mM, ideal for monitoring patients with elevated urea levels, such as those suffering from renal dysfunction. *Ex vivo* tests on porcine and mouse skin demonstrated the device's effectiveness for continuous urea monitoring, with high stability and biocompatibility [264]. The same author presented the development of a protective layer polymeric MNA (PL-pMNA) biosensor platform, which combined a protective PL membrane Fig. 5C_1–C_4 with a gold-coated MNA structure (Au-pMNA**)** Fig. 5C_5–C_{10}. Using 3D-printing and soft lithography technologies, this platform allowed the development of complex biosensor surfaces. The gold layer provided a conductive surface for electrochemical measurements, while the PL membrane protected the biosensor during skin insertion. The platform was tested for glucose and insulin detection, with a linear range of 0.5–21 mM for glucose and 0.2–2 nM for insulin, covering relevant levels for monitoring in healthy individuals and diabetic patients. Tests on porcine skin showed that the PL membrane protected the sensor layer during insertion, keeping stable electrochemical response and preventing damage to the biosensor [284].

5. 3D printing MNs for sensors applied to agriculture and environment

One of the major global concerns for the coming decades is related to agriculture and the challenges and constraints related to food security and food safety. According to FAO projections, a 70% increase in global food production will be required to ensure that the world's population, estimated to reach 9.1 billion people by 2050, can have access to safe food. It is noteworthy that, in developing countries, production will need to double [286]. In addition to increasing food production, strategies to reduce food losses caused by plant diseases and logistical challenges will also be necessary. When infected by pathogens, commercially important plants exhibit a significant reduction in food quality and productivity [287]. Diseases caused by viruses, fungi, and bacteria are estimated to result in annual losses of 20% in global agricultural production [288]. This corresponds to an estimated economic loss of US$ 220 billion per year [289]. Therefore, using technologies capable of early detection and diagnosis of these diseases is essential for effective management and implementing more cost-effective control measures [290].

In this context, the scientific community points to the need for implementing Agriculture 5.0. This concept refers to the advanced integration of digital technologies, such as artificial intelligence, the Internet of Things (IoT), and automation, to optimize production sustainably and

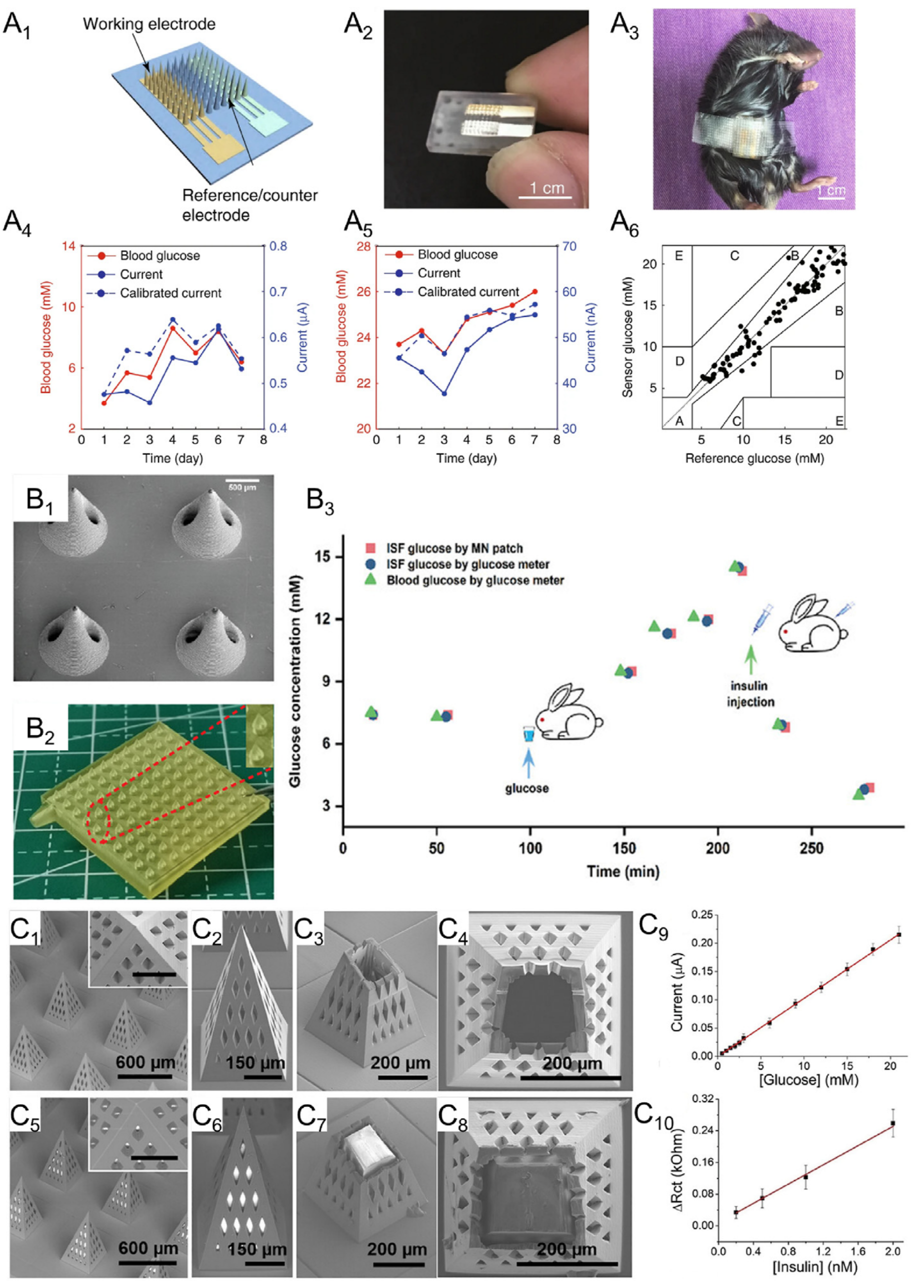

Fig. 5. (A_1) Schematic representation of MNA produced by DLP printing, integrated to electrodes. In (A_2) is shown the photograph image of the printed device, integrated to the electrodes, and in (A_3) an image of the MNA applied to a mouse. (A_4) Seven-day monitoring of subcutaneous glucose levels in a normal mouse using the MN biosensor device (blue) compared to a commercial device (red). (A_5) Seven-day monitoring of subcutaneous glucose levels in a diabetic mouse using the MN biosensor device (blue), compared to a commercial device (red). (A_6) Clark error grid for the MN biosensor device. The x-axis represents blood glucose reference values measured by a commercial glucose meter, and the y-axis shows glucose values measured by the MN biosensor device, image adapted with permission of Liu et al. [256] Copyright 2021, Nature. In (B_1) is shown a SEM image of hollow MN produced by SLA printing, and in (B_2) a digital photograph of the printed array. (B_3) Comparison of glucose measurements in interstitial fluid obtained with MAP (red cube) and glucometer (purple dot) in relation to venous blood glucose concentrations measured with a glucometer (green triangle). Image adapted from Xie et al. [283] Copyright 2024, Wiley. (C_1–C_4) SEM images of PL membrane produced by TPP printing. (C_5–C_{10}) PL-pMNA electrode, image adapted from Ref. [284] Copyright 2024, Wiley.

reduce the use of natural resources [291,292]. In this regard, it is believed that the use of sensors applied to agriculture is a strategy of great interest. Electronic and optical devices can provide valuable data on plant health and nutrition through in situ monitoring [290,293–295]. Such information can be used in crop management, leading to significant improvements in the production system [14,61]. This section will address the use of MNs as sensors, or in combination with sensors and therapeutic delivery applied to crop and plant monitoring. The main strategies used for the fabrication of MNs, the most commonly employed materials, the transduction mechanisms involved, as well as emerging trends in this research field, are also discussed.

As discussed before, MNs were initially designed for medical applications, but more recently, they have expanded their applications, including to the agricultural sector [14]. However, some considerations must be contemplated towards the adaptation from biomedical application to agriculture and environment fields. MNs are not typically exposed to environmental stressors (e.g., UV light, humidity, or fluctuating temperatures), which can potentially accelerate the degradation of their compounds and components. Also, for agricultural and environmental applications, the final devices may require greater mechanical strength and resistance to environmental and microbial degradation. Unlike human skin, plants have diverse anatomical structures to which MNs can be applied and anchored. The main plant structures that can be targeted for these applications include roots, stems, and leaves as displayed in Fig. 6A [296]. To absorb water and mineral nutrients from the soil, roots play a crucial role in extracting them. In addition, roots anchor and attach the plant to the soil or other structures, such as climbing plants [296,297]. The stem's function is to connect the roots and leaves, raising them towards the light. Leaves are the main photosynthetic organs of the plant, and to do so they must receive appropriate amounts of sunlight [296,297]. Within plants, as in animals, there is a vascular system responsible for the distribution of fluids, composed of two types of tissue: xylem and phloem. Xylem is related to the conduction of water and inorganic nutrients and storing some substances. This transport occurs from the root's

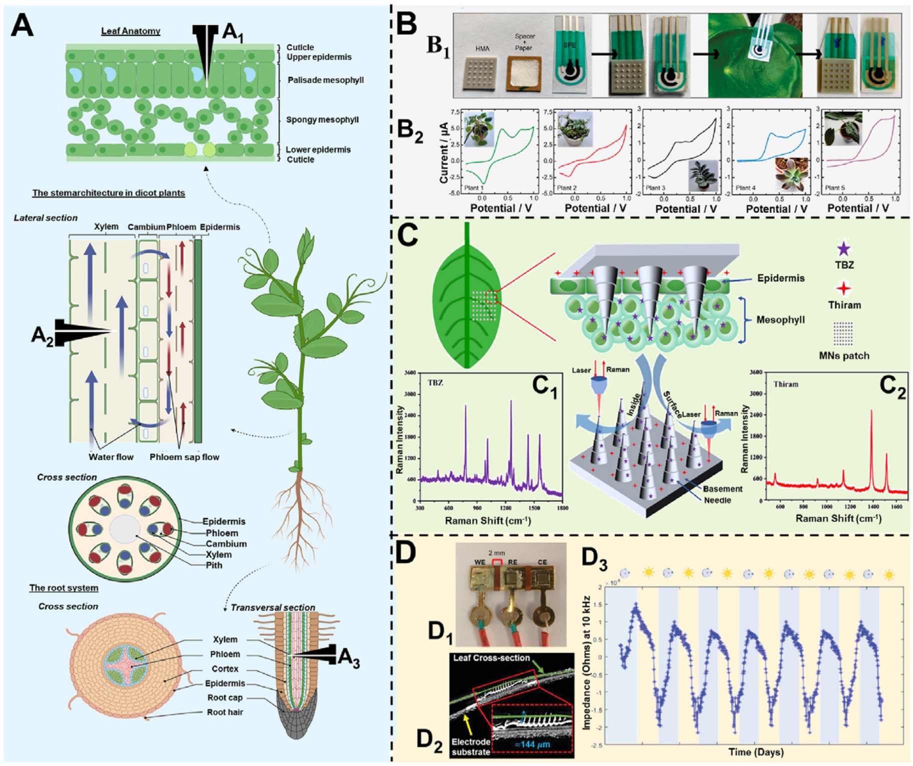

Fig. 6. (A) Plant anatomy and structural presentation of roots, stems, and leaves. (A_1, A_2, A_3), and demonstration of MN. Adopted under the terms of the CC-BY 4.0 license [297]. Copyright 2021, American Chemical Society. (B) *In situ* monitoring of plant health via MN-based sampling device coupled to an electrochemical sensor. (B_1) Device construction illustration showing the device components and field tests. (B_2) Evaluation of device capability to profile plants through cyclic voltammetry (CV) in five different plant species. Reprinted with permission [298]. Copyright 2021, Elsevier. (C) Schematic showing the simultaneous detection of pesticide residues on the surface and within leaves using MNs. (C_1, C_2) Raman images of spectra for two pesticides detected via SERS sensors combined with MNs. Adopted with permission from Ref. [57] Copyright 2023, American Chemical Society. (D) Impedance sensor applied to plants. (D_1) Sensor equipped with MNs showing the arrangement of the working electrode (WE), reference electrode (RE) and counter electrode (CE). (D_2) Cross-sectional 3D X-ray image of the MNs inserted into the leaf. (D_3) Impedance values detected by the sensors equipped with MNs over 7 d for an Arabidopsis thaliana specimen under natural light or in the absence of light. Adopted under the terms of the CC-BY 4.0 license [299]. Copyright 2021, Advanced Science published by Wiley-VCH GmbH.

direction to the plants' upper parts. In contrast, phloem is involved in transporting organic substances and water [296,297].

Plant biological fluids contain a variety of molecules, such as plant hormones, nucleic acids (DNA/RNA), metabolites, enzymes, vitamins, and ions, which can serve as markers for the detection of biotic and abiotic stresses [296,297,300]. Through the vascular system, which extends throughout the plant, MNs can be used to access these fluids and, by employing different analytical techniques, they can be utilized to diagnose plant health [14,297]. In addition to their use as sensory devices for plants, MNs can also be employed for the therapeutic delivery of agents aimed at combating pathogens related to specific diseases, or for the administration of nutrients in cases of plant malnutrition [14].

5.1. Agricultural application of 3D printed MNs

As highlighted in previous reviews [14,61], few studies explore the use of MNs in agriculture, either as diagnostic sensors or to deliver essential molecules to plants. Refining the search to MNs produced through additive techniques, such as 3D printing, a significant decrease in the number of published articles is verified. Until now, less than ten articles reported the fabrication of MNs through 3D printing and their testing in plants. Table 2 details relevant data, including the target crop, plant structure, target molecule, fabrication method, material used, needle size, transduction method, LOD or release rate. In this direction, Parrilla et al. [298] used a DLP printer to produce hollow MNs from polymer-based resin. The MNs measured 0.8 mm in diameter and 1 mm in height and were later combined with sensors. The MN openings allowed the extraction of up to 13 μL of biological fluids from the leaves of five plant species (*Pilea peperomioides*, *Curio rowleyanus*, *Zamioculcas zamiifolia*, *Echeveria Raindrops*, and *Alocasia Yucatan Princess)*. The sensors, fabricated on paper using a semi-automatic screen-printing machine, included a carbon-based working electrode, a counter electrode, and a pseudo-Ag/AgCl reference electrode on a polyester film (Fig. 6B_1). Integrating the MNs with the sensor facilitated *in situ* electrochemical analysis of plant health biomarkers, including hydrogen peroxide, glucose, and pH (Fig. 6B_2) [298].

In another work, Parrilla et al. developed solid microneedles fabricated via SLA 3D printing for continuous pH monitoring in the range of pH 4 to pH 7 on plant leaves (Hydrangea macrophylla (Hydrangea); Peperomia polybotrya (Peperomia); Pilea peperomioides (Pilea); Coleus sp. (Coleus)). The microneedles were designed with precise dimensions: 300 μm in diameter, 900 μm in height, and 30 μm at the tip. These structures were coated with a layer of gold and silver, forming the WE and RE, respectively. The WE were functionalized with polyaniline (PANI) to provide pH sensitivity, while the RE was coated with a polyvinyl butyral (PVB) membrane to ensure potential stability. The device was validated in two contexts: *ex vivo*, using sap extracted from plants, and *in vivo*, with direct pH monitoring on plant leaves over several days. The device could detect pH variations associated with abiotic stress conditions, such as drought and irrigation [303].

Yi et al. [57] introduced a novel strategy for detecting pesticides on vegetable leaves. The authors developed PVA/HA MNs using two methods: 3D printing and PDMS molding (Fig. 6C). The MNs had a diameter of 470 μm, and a height of 880 μm. For the detection tests, they sprayed different pesticide concentrations onto tea, spinach, and tomato leaves. They then gently inserted the MNs into the leaves and performed detection using surface-enhanced Raman spectroscopy (SERS) with a laser confocal microscope (Fig. 6C_1 and 6C_2). The limits of detection (LOD) for thiram and thiabendazole were found to be 10^{-7} and 10^{-8} M, respectively. The authors concluded that the sensor enabled minimally invasive detection without harming the agricultural products [57].

Chen et al. developed an integrated system for real-time glucose monitoring in plants (stem of tomato and leaf of Aloe vera, respectively) using electrochemical sensors based on hollow MNs. The device combines polymeric MNs fabricated via SLA 3D printing, with dimensions of 6 mm × 6 mm, 2 mm in height, and 300 μm in base diameter, along with platinum electrodes modified with gold nanoparticles, Nafion, glucose oxidase, and polyurethane (MPt-AuNPs-Nafion-GOx-Pu). In situ measurements were conducted over a 12 h period, detecting variations in glucose levels during diurnal and overnight cycles. Under saline stress conditions, glucose synthesis was inhibited due to reduced photosynthesis. The sensor was evaluated across a range of glucose concentrations,

Table 2
Examples of MN-based sensors applied to plants.

Target crop	Plant structure	Target molecule	Fabrication method	Material used	Needle size	Transduction method	LOD	Ref.
Pilea pepermioides, Curio rowleyanus, Zamioculcas zamiifolia, Echeveria Raindrops, and Alocasia Yucatan Princess	Leaves	pH, H_2O_2, and glucose	3D printer by stereolithography (SLA)	Polymer resin Snow Gray 8K	Diameter of 0.6/ 0.8 mm, and height of 1.00 mm	Electrochemical	ND	[298]
Tea, spinach and tomato	Leaves	Thiram and thiabendazole pesticide	3D printing and PDMS	Poly(vinyl alcohol) and sodium hyaluronate	Diameter of 470 μm, and height of 880 μm	Surface enhanced Raman spectroscopy	10^{-7}th 10^{-8} M	[57]
Arabidopsis thaliana	Leaves	Water	3D printing by two-photon polymerization (TPP) and PDMS	Titanium and gold.	Diameter of 70 μm and height of 400 μm	Electrical impedance spectroscopy	ND	[299]
Barley	Leaves	Water	3D printing by two-photon polymerization (TPP) and PDMS	Titanium, nickel and gold.	Diameter of 240 μm and height of 230 μm	Bioimpedance	ND	[301]
Target crop	**Plant of structure**	**Released molecule**	**Fabrication method**	**Material used**	**Needle size**	**Disease**	**Released content**	**Ref**
Valencia orange	Stem	Cu nanoparticle	3D printing by digital light processing (DLP)	Polymer resin	Diameter of 375 μm and height of 1000 μm	Huanglongbing	2.2 mg/mL in 24 h	[302]

achieving a detection limit of 33.3 μM and a sensitivity of 17 nA/μM·cm^2, with a detection range spanning from 100 μM to 100 mM. Furthermore, the device exhibited excellent biocompatibility, with complete plant wound healing observed within 15 d, showing no signs of necrosis or significant damage [304].

In another approach, Bukhamsin et al. [299] developed impedimetric sensors using MNs to monitor plant stress factors such as light and hydration levels. The MNs were created using a PDMS mold produced by 3D printing with TPP. This PDMS mold then facilitated the production of polyimide MNs. Following this, the MNs were placed on a silicon substrate coated with an uncured polyimide layer, which was heated to 350 °C to secure the MNs through crosslinking. A CO_2 laser shaped the film into the desired electrode bed, and the film was then detached to retain its flexibility. To achieve electrical conductivity, the MNs were coated with a layer of titanium and gold (Fig. 6D). A laser-cut polymethyl methacrylate (PMMA) shadow mask ensured precise 2 mm spacing between each MN-equipped electrode (Fig. 6D_1). Plant tests involved the application of MNs to the leaves of *Arabidopsis thaliana* (Fig. 6D_2). The authors observed significant impedance variations in response to differing light and hydration levels (Fig. 6D_3). Additionally, when comparing MN-based devices with conventional planar sensors, results showed that MN sensors offered enhanced sensitivity, detecting subtle and discernible changes in the physiological state of the plant tissue. This improved sensitivity underscores the potential of MNs for accurately monitoring plant physiological stress responses.

In a previous study, Bukhamsin et al. [299] developed an impedimetric sensor based on flexible MNs. The MNs were fabricated similarly to their prior work, with a modification: the needles received titanium, nickel, and gold coatings to enhance conductive properties. The sensor utilized bioimpedance as a transduction method to evaluate plant responses to variations in light exposure and temperature. For testing, barley plants were grown in controlled chambers with 12-h light cycles at 22 °C and darkness at 16 °C. Bioimpedance measurements of the leaves were recorded across frequencies from 1 Hz to 100 kHz using a portable potentiostat (PalmSens4, PalmSens BV). Results indicated that bioimpedance increased significantly in light conditions and decreased in darkness. This variation was linked to water movement within the leaves; during the day, photosynthesis promotes a constant water flow to the leaves, raising impedance, while at night, the osmotic balance between the leaf and stem reduces water movement, consequently lowering bioimpedance.

Santra et al. [302] report the only study utilizing 3D-printed MNs for delivering essential substances directly to plants. Citrus plantations can be severely impacted by the bacterium *Candidatus Liberibacter asiaticus*, which resides exclusively within the phloem of citrus plants, causing significant crop losses. Conventional disease management approaches, primarily foliar applications, are ineffective for targeting the phloem. Using a DLP 3D printer, they fabricated a set of MNs enabling copper delivery directly to the phloem as a treatment strategy. Specifically, copper nanoparticles were emulsified with sodium oleate to facilitate binding between the hydrophobic MN resin and the water within the phloem. This copper nanoparticle coating was applied to the MNs via a spin-coating process, providing a targeted approach to combat the infection. The authors observed that the MNs demonstrated effective penetration into the plant stems. Release assays conducted in water showed that the MNs successfully delivered 100% of the Cu nanoparticles within 24 h, reaching an approximate concentration of 2.2 mg/mL. This release profile suggests a potential for controlled, slow-release kinetics for effective bacterial control in plants.

6. Conclusion and final remarks

MNs and MNAs manufactured by 3D printing are potential materials that have enabled remarkable scientific and technological advances. These innovative devices have already demonstrated their versatility in areas such as transdermal drug delivery, vaccine administration, and fluid sampling for clinical analysis and diagnostics. Additionally, their utility has extended to veterinary and botanical applications.

Recent progress in additive manufacturing has revolutionized the fabrication of MNs using 3D-printing, enabling a fast and cost-effective process that utilizes polymer-based materials. This scenario has also catalyzed the development of biopolymer-based resins, opening avenues for sustainable and biocompatible solutions. Among the distinct 3D-printing techniques, those that explore VAT polymerization have been the most used for customized high-resolution MN-based devices. FDM still presents limitations regarding temperature gradient, time of printing, biocompatibility of the materials, and low resolution of the MNs. While CLIP is a technique able to enable improvements in printing resolution, it is still few explored for printing of MN, which suggests space for new researches endeavors. However, MNs could evolve beyond this function to serve as fully integrated sensors.

While electroanalytical analysis has been traditionally explored in MN-based sensors, easy-to-interpret colorimetric (bio)sensors are promising. In this way, numerous researches demonstrate the efficient integration of MNs to wearable platforms for the detection of biomarkers for healthcare and agriculture interests. While the application of MNs in plants is still embryonic, preliminary studies indicate substantial potential for growth in this area.

The scientific literature reports that the advances of the (bio)sensors' field have been efficiently transposed to MN-based sensors, with the possibility of simultaneous detection of multiple analytes, integration of microfluidic devices, biocompatibility, and successful application *in vivo* models, particularly when paired with novel functional materials and methods. Key future research developments in 3D-printed MNs' include the creation of biobased resins, and biocompatible photoinitiators, as well as the incorporation of nanomaterials to improve the mechanical properties and provide additional functionalities for the customized MNs.

Although MNAs have been successfully implemented, regulatory approval remains crucial for MNAs market adoption. Compliance with good manufacturing practices and quality regulations, as outlined by the FDA and the Center for Devices and Radiological Health (CDRH), the Center for Drug Evaluation and Research (CDER), and the Center for Biologics Evaluation and Research (CBER) [305] is essential to ensure the safety and efficacy of these products. Particular focus must be given to biocompatibility, sterilization, and validation, especially when they are intended living organisms. Any chemical changes to the materials or degradation products resulting from repeated melting, cooling cycles, or photopolymerization must be anticipated, identified, and addressed. Furthermore, the stability and chemical behavior of drugs and active compounds incorporated into the polymer matrix must be validated under various 3D printing conditions, such as exposure to high temperatures, radiation, and other physicochemical alterations. These measures are vital to ensure consistent performance, prevent contamination and toxicity, and maintaining traceability throughout the product lifecycle. This is expected to be reached in the near future, considering the experience and technology gained with cosmetic MNs already available on the market.

In summary, 3D-printed MNs represent a rapidly evolving field with vast potential for technological innovation. By addressing existing challenges and exploring interdisciplinary applications, this technology is poised to make groundbreaking contributions to biomedicine, agriculture, environmental monitoring and beyond in the next years.

CRediT authorship contribution statement

Kelcilene B.R. Teodoro: Writing – original draft, Methodology, Conceptualization. **Tamires S. Pereira:** Writing – original draft, Methodology. **Ana Laura M.M. Alves:** Writing – original draft, Methodology. **Francisco V. dos Santos:** Writing – original draft, Methodology. **Fabrício A. dos Santos:** Writing – original draft, Methodology. **Daniel S. Correa:** Writing – review & editing, Supervision, Project administration, Conceptualization.

Declaration of competing interest

The authors declare that they have no known competing financial interests or personal relationships that could have appeared to influence the work reported in this paper.

Acknowledgments

The authors thank the financial support from Fundação de Amparo à Pesquisa do Estado de São Paulo (FAPESP) (Grant numbers: 2022/09686-1, 2020/10048–4, 2022/05316–5, 2023/01567–6, 2023/13428–0), Conselho Nacional de Desenvolvimento Científico e Tecnológico (CNPq) and Coordenação de Aperfeiçoamento de Pessoal de Nível Superior - Brasil (CAPES) - Código de Financiamento 001.

References

[1] H. Islam, T.S. Poly, Z.T. Tisha, S. Rahman, A.I.J. Naveed, A. Ahmed, S.N. Ahmed, J. Hassan, MdJ. Uddin, D.B. Das, 3D printed hollow microneedles for treating skin Wrinkles using different anti-wrinkle agents: a possible futuristic approach, Cosmetics 10 (2) (2023) 41, https://doi.org/10.3390/cosmetics10020041.

[2] S.H. Lim, H. Kathuria, M.H. Bin Amir, X. Zhang, H.T.T. Duong, P.C.-L. Ho, L. Kang, High resolution photopolymer for 3D printing of personalised microneedle for transdermal delivery of anti-wrinkle small peptide, J. Contr. Release 329 (2021) 907, https://doi.org/10.1016/j.jconrel.2020.10.021.

[3] C. Caudill, J.L. Perry, K. Iliadis, A.T. Tessema, B.J. Lee, B.S. Mecham, S. Tian, J.M. DeSimone, Transdermal vaccination via 3D-printed microneedles induces potent humoral and cellular immunity, Proc. Natl. Acad. Sci. USA 118 (39) (2021) e2102595118, https://doi.org/10.1073/pnas.2102595118.

[4] B. Ciui, A. Martin, R.K. Mishra, B. Brunetti, T. Nakagawa, T.J. Dawkins, M. Lyu, C. Cristea, R. Sandulescu, J. Wang, Wearable wireless Tyrosinase Bandage and microneedle sensors: toward melanoma screening, Adv. Healthcare Mater. 7 (2018) 1701264, https://doi.org/10.1002/adhm.201701264.

[5] C. Moonla, M. Reynoso, A. Casanova, A.Y. Chang, O. Djassemi, A. Balaje, A. Abbas, Z. Li, K. Mahato, J. Wang, Continuous ketone monitoring via wearable microneedle patch platform, ACS Sens. 9 (2) (2024) 1004, https://doi.org/10.1021/acssensors.3c02677.

[6] P.V.A. Gerstel M. S., Drug delivery device (1976). Patent US3964482A.

[7] L. Wang, Y. Wang, X. Wu, P. Wang, X. Luo, S. Lv, Advances in microneedles for transdermal diagnostics and sensing applications, Microchim. Acta 191 (2024) 406, https://doi.org/10.1007/s00604-024-06458-2.

[8] K.J. Lee, S.S. Jeong, D.H. Roh, D.Y. Kim, H.-K. Choi, E.H. Lee, A practical guide to the development of microneedle systems – in clinical trials or on the market, Int. J. Pharm. 573 (2020) 118778, https://doi.org/10.1016/j.ijpharm.2019.118778.

[9] P. Singh, A. Carrier, Y. Chen, S. Lin, J. Wang, S. Cui, X. Zhang, Polymeric microneedles for controlled transdermal drug delivery, J. Contr. Release 315 (2019) 97, https://doi.org/10.1016/j.jconrel.2019.10.022.

[10] I. Menon, P. Bagwe, K.B. Gomes, L. Bajaj, R. Gala, M.N. Uddin, M.J. D'Souza, S.M. Zughaier, Microneedles: a new generation vaccine delivery system, Micromachines 12 (4) (2021) 435, https://doi.org/10.3390/mi12040435.

[11] J.J. García-Guzmán, C. Pérez-Ràfols, M. Cuartero, G.A. Crespo, Microneedle based electrochemical (Bio)Sensing: towards decentralized and continuous health status monitoring, TrAC, Trends Anal. Chem. 135 (2021) 116148, https://doi.org/10.1016/j.trac.2020.116148.

[12] I.-J. Choi, W. Na, A. Kang, M.-H. Ahn, M. Yeom, H.-O. Kim, J.-W. Lim, S.-O. Choi, S.-K. Baek, D. Song, J.-H. Park, Patchless administration of canine influenza vaccine on dog's ear using insertion-responsive microneedles (IRMN) without removal of hair and its in vivo efficacy evaluation, Eur. J. Pharm. Biopharm. 153 (2020) 150, https://doi.org/10.1016/j.ejpb.2020.06.006.

[13] B. Wang, H. Lu, S. Jiang, B. Gao, Recent advances of microneedles biosensors for plants, Anal. Bioanal. Chem. 416 (2024) 55, https://doi.org/10.1007/s00216-023-05003-z.

[14] Z. Faraji Rad, P.D. Prewett, G.J. Davies, Rapid prototyping and customizable microneedle design: ultra-sharp microneedle fabrication using two-photon polymerization and low-cost micromolding techniques, Manuf Lett 30 (2021) 39, https://doi.org/10.1016/J.MFGLET.2021.10.007.

[15] E.D. Ozyilmaz, A. Turan, T. Comoglu, An overview on the advantages and limitations of 3D printing of microneedles, Pharmaceut. Dev. Technol. 26 (2021) 923, https://doi.org/10.1080/10837450.2021.1965163.

[16] N. Elahpour, F. Pahlevanzadeh, M. Kharaziha, H.R. Bakhsheshi-Rad, S. Ramakrishna, F. Berto, 3D printed microneedles for transdermal drug delivery: a brief review of two decades, Int. J. Pharm. 597 (2021) 120301, https://doi.org/10.1016/j.ijpharm.2021.120301.

[17] World Economic Forum, Top 10 Emerging Technologies (2020) Special Report, 2020. https://www3.weforum.org/docs/WEF_Top_10_Emerging_Technologies_2020.Pdf.

[18] V. Gambardella, N. Tarazona, J.M. Cejalvo, P. Lombardi, M. Huerta, S. Roselló, T. Fleitas, D. Roda, A. Cervantes, Personalized medicine: recent progress in cancer therapy, Cancers 12 (4) (2020) 1009, https://doi.org/10.3390/cancers12041009.

[19] Z. Li, S. Kadian, R.K. Mishra, T. Huang, C. Zhou, S. Liu, Z. Wang, R. Narayan, Z. Zhu, Electrochemical detection of cholesterol in human biofluid using microneedle sensor, J. Mater. Chem. B 11 (2023) 6075, https://doi.org/10.1039/D2TB02142K.

[20] K.Y. Goud, C. Moonla, R.K. Mishra, C. Yu, R. Narayan, I. Litvan, J. Wang, Wearable electrochemical microneedle sensor for continuous monitoring of Levodopa: toward Parkinson management, ACS Sens 4 (8) (2019) 2196, https://doi.org/10.1021/acssensors.9b01127.

[21] A. Bukhamsin, A. Ait Lahcen, J.D.O. Filho, S. Shetty, I. Blilou, J. Kosel, K.N. Salama, Minimally-invasive, real-time, non-destructive, species-independent

phytohormone biosensor for precision farming, Biosens. Bioelectron. 214 (2022) 114515, https://doi.org/10.1016/j.bios.2022.114515.
[22] D. Álvarez-Muñoz, M. Farré, A snapshot of biomarkers of exposure for environmental monitoring, in: Environmental Metabolomics: Applications in Field and Laboratory Studies to Understand from Exposome to Metabolome, Elsevier, 2020, p. 311, https://doi.org/10.1016/B978-0-12-818196-6.00011-X.
[23] A. Kaidarova, N.R. Geraldi, R.P. Wilson, J. Kosel, M.G. Meekan, V.M. Eguíluz, M.M. Hussain, A. Shamim, H. Liao, M. Srivastava, S.S. Saha, M.S. Strano, X. Zhang, B.S. Ooi, M. Holton, L.W. Hopkins, X. Jin, X. Gong, F. Quintana, A. Tovasarov, A. Tasmagambetova, C.M. Duarte, Wearable sensors for monitoring marine environments and their inhabitants, Nat. Biotechnol. 41 (2023) 1208, https://doi.org/10.1038/s41587-023-01827-3.
[24] A. Zarnegar, Point-of-Care Devices in Healthcare: A Public Health Perspective, In: Daimi, K., Alsadoon, A., Seabra Dos Reis, S. (eds) Current and Future Trends in Health and Medical Informatics. Studies in Computational Intelligence, 1112 (2023). Springer, Cham. https://doi.org/10.1007/978-3-031-42112-9_4
[25] V. Mazzaracchio, R. Vitiello, G. Maccauro, F. Arduini, Point-of-care devices for the detection of biomarkers of periprosthetic joint infection: state of the art and future perspectives, TrAC, Trends Anal. Chem. 172 (2024) 117544, https://doi.org/10.1016/j.trac.2024.117544.
[26] G. Adedokun, M. Alipanah, Z.H. Fan, Sample preparation and detection methods in point-of-care devices towards future at-home testing, Lab Chip 24 (2024) 3626, https://doi.org/10.1039/D3LC00943B.
[27] K. Wang, X. Meng, X. Yan, K. Fan, Nanozyme-based point-of-care testing: revolutionizing environmental pollutant detection with high efficiency and low cost, Nano Today 54 (2024) 102145, https://doi.org/10.1016/j.nantod.2023.102145.
[28] B. Heidt, W. Siqueira, K. Eersels, H. Diliën, B. van Grinsven, R. Fujiwara, T. Cleij, Point of care diagnostics in resource-limited settings: a review of the present and future of PoC in its most needed environment, Biosensors 10 (10) (2020) 133, https://doi.org/10.3390/bios10100133.
[29] H.N. Nayan Kumar, D.H. Nagaraju, Z. Yhobu, P. Shivakumar, K.S. Manjunatha Kumara, S. Budagumpi, B.M. Praveen, Recent advances in on-site monitoring of heavy metal ions in the environment, Microchem. J. 182 (2022) 107894, https://doi.org/10.1016/j.microc.2022.107894.
[30] A. Rani, V.B. Ravindran, A. Surapaneni, N. Mantri, A.S. Ball, Review: trends in point-of-care diagnosis for Escherichia coli O157:H7 in food and water, Int. J. Food Microbiol. 349 (2021) 109233, https://doi.org/10.1016/j.ijfoodmicro.2021.109233.
[31] H. Sohrabi, M.R. Majidi, P. Khaki, A. Jahanban-Esfahlan, M. de la Guardia, A. Mokhtarzadeh, State of the art: lateral flow assays toward the point-of-care foodborne pathogenic bacteria detection in food samples, Compr. Rev. Food Sci. Food Saf. 21 (2022) 1868, https://doi.org/10.1111/1541-4337.12913.
[32] Z. Suo, X. Niu, M. Wei, H. Jin, B. He, Latest strategies for rapid and point of care detection of mycotoxins in food: a review, Anal. Chim. Acta 1246 (2023) 340888, https://doi.org/10.1016/j.aca.2023.340888.
[33] D. Kim, Y. Cao, D. Mariappan, M.S. Bono, A.J. Hart, B. Marelli, A microneedle technology for sampling and sensing bacteria in the food supply chain, Adv. Funct. Mater. 31 (1) (2021) 2005370, https://doi.org/10.1002/adfm.202005370.
[34] P. Baldi, N. La Porta, Molecular approaches for low-cost point-of-care pathogen detection in agriculture and forestry, Front. Plant Sci. 11 (2020) 570862, https://doi.org/10.3389/fpls.2020.570862.
[35] A. Pal, S.K. Dubey, S. Goel, P.K. Kalita, Portable sensors in precision agriculture: assessing advances and challenges in soil nutrient determination, TrAC, Trends Anal. Chem. 180 (2024) 117981, https://doi.org/10.1016/j.trac.2024.117981.
[36] A. Merkoçi, Smart nanobiosensors in agriculture, Nat Food 2 (2021) 920, https://doi.org/10.1038/s43016-021-00426-2.
[37] N. Amin, A. Almasi, T. Ozer, C.S. Henry, L. Hosseinzadeh, Z. Keshavarzi, Recent advances of optical biosensors in veterinary medicine: moving towards the point of care applications, Curr. Top. Med. Chem. 23 (2023) 2242, https://doi.org/10.2174/1568026623666230718163613.
[38] L. Wang, Z. Zhou, J. Niu, J. Peng, T. Wang, X. Hou, Emerging innovations in portable chemical sensing devices: advancements from microneedles to hydrogel, microfluidic, and paper-based platforms, Talanta 278 (2024) 126412, https://doi.org/10.1016/j.talanta.2024.126412.
[39] S. Kadian, P. Kumari, S.S. Sahoo, S. Shukla, R.J. Narayan, Machine learning enabled microneedle-based colorimetric pH sensing patch for wound health monitoring and meat spoilage detection, Microchem. J. 200 (2024) 110350, https://doi.org/10.1016/j.microc.2024.110350.
[40] H. Sun, S. Wang, H. Wang, Q. Zeng, F. Wang, Y. Zheng, H. Haick, G. Shi, M. Zhang, Stick-and-sensing microneedle patch for personalized nutrition management, Sens Actuators B Chem 418 (2024) 136207, https://doi.org/10.1016/j.snb.2024.136207.
[41] M. Shikida, et al., Fabrication of pen-shaped microneedle structure by using non-photolithographic pattern transfer 2 (2003) 1671, https://doi.org/10.1109/SENSOR.2003.1217104.
[42] M. Shikida, M. Ando, Y. Ishihara, T. Ando, K. Sato, K. Asaumi, Non-photolithographic pattern transfer for fabricating pen-shaped microneedle structures, J. Micromech. Microeng. 14 (2004) 1462, https://doi.org/10.1088/0960-1317/14/11/005.
[43] X.P. Zhang, B.L. Zhang, B.Z. Chen, Z.Q. Zhao, W.M. Fei, Y. Cui, X.D. Guo, Dissolving microneedle rollers for rapid transdermal drug delivery, Drug Deliv Transl Res 12 (2022) 459, https://doi.org/10.1007/s13346-021-01048-8.
[44] A. Omolu, M. Bailly, R.M. Day, Assessment of solid microneedle rollers to enhance transmembrane delivery of doxycycline and inhibition of MMP activity, Drug Deliv. 24 (2017) 942, https://doi.org/10.1080/10717544.2017.1337826.
[45] S.-Y. Jeong, Y.-S. Lee, J.-Y. Park, J.-H. Park, H.-J. Park, S.-Y. Kim, Designing a placebo microneedle stamp: modeling and validation in a clinical control trial, Pharmaceutics 16 (2024) 395, https://doi.org/10.3390/pharmaceutics16030395.
[46] S.-Y. Jeong, J.-Y. Park, Y.-S. Kim, S.-Y. Kim, Contemporary application of roller needle and stamp needle: a patent review, Korean Journal of Acupuncture 36 (2019) 139, https://doi.org/10.14406/acu.2019.017.
[47] U.O. Häfeli, A. Mokhtari, D. Liepmann, B. Stoeber, In vivo evaluation of a microneedle-based miniature syringe for intradermal drug delivery, Biomed. Microdevices 11 (2009) 943, https://doi.org/10.1007/s10544-009-9311-y.
[48] B. O'Flynn, M. De Donno, C. Barrett, C. Robinson, A.O. Riordan, Smart microneedle sensing systems for security in agriculture, food and the environment (SAFE). 2017 IEEE SENSORS, IEEE, 2017, pp. 1–3, https://doi.org/10.1109/ICSENS.2017.8233884.
[49] R. Omar, Y. Zheng, J. Wang, H. Haick, Microneedle sensors for multiplex applications: toward advanced biomedical and environmental analysis, Advanced Sensor Research 2 (2) (2023) 2200032, https://doi.org/10.1002/adsr.202200032.
[50] Y. Hu, E. Chatzilakou, Z. Pan, G. Traverso, A.K. Yetisen, Microneedle sensors for point-of-care diagnostics, Adv. Sci. 11 (12) (2024) 2306560, https://doi.org/10.1002/advs.202306560.
[51] K.B.R. Teodoro, F.L. Migliorini, M.H.M. Facure, R.C. Sanfelice, D. Martins, D.S. Correa, Novel chemical sensors based on green composite materials for environmental analysis, Nanosensors for Environment, Food and Agriculture 1 (2021) 109, https://doi.org/10.1007/978-3-030-63245-8_5.
[52] Ö. Erdem, I. Eş, G.A. Akceoglu, Y. Saylan, F. Inci, Recent advances in microneedle-based sensors for sampling, diagnosis and monitoring of chronic diseases, Biosensors 11 (9) (2021) 296, https://doi.org/10.3390/bios11090296.
[53] M. Dalvi, P. Kharat, P. Thakor, V. Bhavana, S.B. Singh, N.K. Mehra, Panorama of dissolving microneedles for transdermal drug delivery, Life Sci 284 (2021) 119877, https://doi.org/10.1016/j.lfs.2021.119877.
[54] Y. Cheng, X. Gong, J. Yang, G. Zheng, Y. Zheng, Y. Li, Y. Xu, G. Nie, X. Xie, M. Chen, C. Yi, L. Jiang, A touch-actuated glucose sensor fully integrated with microneedle array and reverse iontophoresis for diabetes monitoring, Biosens. Bioelectron. 203 (2022) 114026, https://doi.org/10.1016/J.BIOS.2022.114026.
[55] Y. Tian, J. Lee, K. van der Maaden, Y. Bhide, J.J. de Vries-Idema, R. Akkerman, C. O'Mahony, W. Jiskoot, H.W. Frijlink, A.L.W. Huckriede, W.L.J. Hinrichs, J.A. Bouwstra, M. Beukema, Intradermal administration of influenza vaccine with trehalose and pullulan-based dissolving microneedle arrays, J. Pharmaceut. Sci. 111 (2022) 1070, https://doi.org/10.1016/j.xphs.2022.01.033.
[56] R. Paul, A.C. Saville, J.C. Hansel, Y. Ye, C. Ball, A. Williams, X. Chang, G. Chen, Z. Gu, J.B. Ristaino, Q. Wei, Extraction of plant DNA by microneedle patch for rapid detection of plant diseases, ACS Nano 13 (6) (2019) 6540, https://doi.org/10.1021/acsnano.9b00193.
[57] X. Yi, Z. Yuan, X. Yu, L. Zheng, C. Wang, Novel microneedle patch-based surface-enhanced Raman spectroscopy sensor for the detection of pesticide residues, ACS Appl. Mater. Interfaces 15 (4) (2023) 4873, https://doi.org/10.1021/acsami.2c17954.
[58] A. Ullah, M. Jang, H. Khan, H.J. Choi, S. An, D. Kim, Y.R. Kim, U.K. Kim, G.M. Kim, Microneedle array with a pH-responsive polymer coating and its application in smart drug delivery for wound healing, Sens Actuators B Chem 345 (2021) 130441, https://doi.org/10.1016/J.SNB.2021.130441.
[59] M. Ravindra Babu, S. Vishwas, M. Gulati, K. Dua, S. Kumar Singh, Harnessing the role of microneedles as sensors: current status and future perspectives, Drug Discov. Today 29 (2024) 104030, https://doi.org/10.1016/J.DRUDIS.2024.104030.
[60] F.K. Aldawood, A. Andar, S. Desai, A comprehensive review of microneedles: types, materials, processes, characterizations and applications, Polymers 13 (16) (2021) 2815, https://doi.org/10.3390/polym13162815.
[61] E. Ece, I. Eş, F. Inci, Microneedle technology as a new standpoint in agriculture: treatment and sensing, Mater. Today 68 (2023) 275, https://doi.org/10.1016/j.mattod.2023.07.002.
[62] S.M. Mugo, S.V. Robertson, M. Wood, A hybrid stainless-steel SPME microneedle electrode sensor for dual electrochemical and GC-MS analysis, Sensors 23 (2023) 2317, https://doi.org/10.3390/s23042317.
[63] Y. Cheng, X. Luan, J. Weng, L. Zhang, F. Ye, Engineering sampling microneedles for biomolecules sensing, Chem. Eng. J. 499 (2024) 156130, https://doi.org/10.1016/J.CEJ.2024.156130.
[64] D. Al Sulaiman, J.Y.H. Chang, N.R. Bennett, H. Topouzi, C.A. Higgins, D.J. Irvine, S. Ladame, Hydrogel-coated microneedle arrays for minimally invasive sampling and sensing of specific circulating nucleic acids from skin interstitial fluid, ACS Nano 13 (8) (2019) 9620, https://doi.org/10.1021/acsnano.9b04783.
[65] J.R. Windmiller, N. Zhou, M.-C. Chuang, G. Valdés-Ramírez, P. Santhosh, P.R. Miller, R. Narayan, J. Wang, Microneedle array-based carbon paste amperometric sensors and biosensors, Analyst 136 (2011) 1846, https://doi.org/10.1039/c1an00012h.
[66] C. Zhan, F. Liu, Z. Shen, X. Huang, S. Huang, X. Li, J. Liu, J. Yang, J. Xu, X. Xie, H.J. Chen, A 3D-printed microneedle extraction system integrated with patterned electrodes for minimally invasive transdermal detection, Biomater. Sci. 11 (2023) 3737, https://doi.org/10.1039/d2bm01975b.
[67] J. Xu, D. Xu, X. Xuan, H. He, Advances of microneedles in biomedical applications, Molecules 26 (2021) 5912, https://doi.org/10.3390/molecules26195912.
[68] S. Yao, C. Zhang, J. Ping, Y. Ying, Recent advances in hydrogel microneedle-based biofluid extraction and detection in food and agriculture, Biosens. Bioelectron. 250 (2024) 116066, https://doi.org/10.1016/j.bios.2024.116066.
[69] I.R. Ausri, S. Sadeghzadeh, S. Biswas, H. Zheng, P. GhavamiNejad, M.D.T. Huynh, F. Keyvani, E. Shirzadi, F.A. Rahman, J. Quadrilatero, A. GhavamiNejad,

M. Poudineh, Multifunctional dopamine-based hydrogel microneedle electrode for continuous ketone sensing, Adv. Mater. 36 (32) (2024) 2402009, https://doi.org/10.1002/adma.202402009.
[70] S. Lyu, Z. Dong, X. Xu, H.P. Bei, H.Y. Yuen, C.W. James Cheung, M.S. Wong, Y. He, X. Zhao, Going below and beyond the surface: microneedle structure, materials, drugs, fabrication, and applications for wound healing and tissue regeneration, Bioact. Mater. 27 (2023) 303, https://doi.org/10.1016/J.BIOACTMAT.2023.04.003.
[71] M.R. Prausnitz, Microneedles for transdermal drug delivery, Adv. Drug Deliv. Rev. 56 (2004) 581, https://doi.org/10.1016/J.ADDR.2003.10.023.
[72] J.H. Park, M.G. Allen, M.R. Prausnitz, Biodegradable polymer microneedles: fabrication, mechanics and transdermal drug delivery, J. Contr. Release 104 (2005) 51, https://doi.org/10.1016/J.JCONREL.2005.02.002.
[73] R. Nagarkar, M. Singh, H.X. Nguyen, S. Jonnalagadda, A review of recent advances in microneedle technology for transdermal drug delivery, J. Drug Deliv. Sci. Technol. 59 (2020) 101923, https://doi.org/10.1016/J.JDDST.2020.101923.
[74] K. Schossleitner, C. O'Mahony, S. Brandstätter, M.J. Haslinger, S. Demuth, D. Fechtig, P. Petzelbauer, Differences in biocompatibility of microneedles from cyclic olefin polymers with human endothelial and epithelial skin cells, J. Biomed. Mater. Res. 107 (2019) 505, https://doi.org/10.1002/JBM.A.36565.
[75] K. Moussi, A. Bukhamsin, T. Hidalgo, J. Kosel, Biocompatible 3D printed microneedles for transdermal, intradermal, and percutaneous applications, Adv. Eng. Mater. 22 (2) (2020) 1901358, https://doi.org/10.1002/adem.201901358.
[76] X. Zhang, C. Zhou, T. Chen, Z. Jiang, C. Lu, C. Wu, X. Pan, Z. Huang, T. Peng, State-of-the-art strategies to enhance the mechanical properties of microneedles, Int. J. Pharm. 663 (2024) 124547, https://doi.org/10.1016/j.ijpharm.2024.124547.
[77] H. Abdullah, T. Phairatana, I. Jeerapan, Tackling the challenges of developing microneedle-based electrochemical sensors, Microchim. Acta 189 (11) (2022) 440, https://doi.org/10.1007/s00604-022-05510-3.
[78] Y. Huang, H. Yu, L. Wang, D. Shen, Z. Ni, S. Ren, Y. Lu, X. Chen, J. Yang, Y. Hong, Research progress on cosmetic microneedle systems: preparation, property and application, Eur. Polym. J. 163 (2022) 110942, https://doi.org/10.1016/j.eurpolymj.2021.110942.
[79] M. Wang, L. Hu, C. Xu, Recent advances in the design of polymeric microneedles for transdermal drug delivery and biosensing, Lab Chip 17 (2017) 1373, https://doi.org/10.1039/C7LC00016B.
[80] Y. Li, X. Hu, Z. Dong, Y. Chen, W. Zhao, Y. Wang, L. Zhang, M. Chen, C. Wu, Q. Wang, Dissolving microneedle arrays with optimized needle geometry for transcutaneous immunization, Eur. J. Pharmaceut. Sci. 151 (2020) 105361, https://doi.org/10.1016/J.EJPS.2020.105361.
[81] Q. Zhou, K. Dong, M. Wei, B. He, B. Gao, Rolling stone gathers moss: rolling microneedles generate meta microfluidic microneedles (MMM), Adv. Funct. Mater. 34 (25) (2024) 2316565, https://doi.org/10.1002/adfm.202316565.
[82] S. Pei, S. Babity, A. Sara Cordeiro, D. Brambilla, Integrating microneedles and sensing strategies for diagnostic and monitoring applications: the state of the art, Adv. Drug Deliv. Rev. 210 (2024) 115341, https://doi.org/10.1016/J.ADDR.2024.115341.
[83] L. Sun, X. Zhu, X. Zhang, G. Chen, F. Bian, J. Wang, Q. Zhou, D. Wang, Y. Zhao, Induced cardiomyocytes-integrated conductive microneedle patch for treating myocardial infarction, Chem. Eng. J. 414 (2021) 128723, https://doi.org/10.1016/J.CEJ.2021.128723.
[84] Y. Huang, H. Li, T. Hu, J. Li, C.K. Yiu, J. Zhou, J. Li, X. Huang, K. Yao, X. Qiu, Y. Zhou, D. Li, B. Zhang, R. Shi, Y. Liu, T.H. Wong, M. Wu, H. Jia, Z. Gao, Z. Zhang, J. He, M. Zheng, E. Song, L. Wang, C. Xu, X. Yu, Implantable electronic medicine enabled by bioresorbable microneedles for wireless electrotherapy and drug delivery, Nano Lett. 22 (14) (2022) 5944–5953, https://doi.org/10.1021/acs.nanolett.2c01997.
[85] S. Zhou, Y. Chino, T. Kasama, R. Miyake, S. Mitsuzawa, Y. Luan, N.B. Ahmad, H. Hibino, M. Takai, Biocompatible core-shell microneedle sensor filled with zwitterionic polymer hydrogel for rapid continuous transdermal monitoring, ACS Nano 18 (39) (2024) 26541, https://doi.org/10.1021/acsnano.4c02997.
[86] K.Y. Goud, K. Mahato, H. Teymourian, K. Longardner, I. Litvan, J. Wang, Wearable electrochemical microneedle sensing platform for real-time continuous interstitial fluid monitoring of apomorphine: toward Parkinson management, Sens Actuators B Chem 354 (2022) 131234, https://doi.org/10.1016/j.snb.2021.131234.
[87] R. Paul, E. Ostermann, Y. Chen, A.C. Saville, Y. Yang, Z. Gu, A.E. Whitfield, J.B. Ristaino, Q. Wei, Integrated microneedle-smartphone nucleic acid amplification platform for in-field diagnosis of plant diseases, Biosens. Bioelectron. 187 (2021) 113312, https://doi.org/10.1016/J.BIOS.2021.113312.
[88] Z. Wang, J. Luan, A. Seth, L. Liu, M. You, P. Gupta, P. Rathi, Y. Wang, S. Cao, Q. Jiang, X. Zhang, R. Gupta, Q. Zhou, J.J. Morrissey, E.L. Scheller, J.S. Rudra, S. Singamaneni, Microneedle patch for the ultrasensitive quantification of protein biomarkers in interstitial fluid, Nature Biomedical Engineering 2021 5 (15) (2021) 64, https://doi.org/10.1038/s41551-020-00672-y.
[89] W. Qin, G. Quan, Y. Sun, M. Chen, P. Yang, D. Feng, T. Wen, X. Hu, X. Pan, C. Wu, Dissolving microneedles with spatiotemporally controlled pulsatile release nanosystem for synergistic chemo-photothermal therapy of melanoma, Theranostics 10 (2020) 8179, https://doi.org/10.7150/THNO.44194.
[90] D.D. Zhu, L.W. Zheng, P.K. Duong, R.H. Cheah, X.Y. Liu, J.R. Wong, W.J. Wang, S.T. Tien Guan, X.T. Zheng, P. Chen, Colorimetric microneedle patches for multiplexed transdermal detection of metabolites, Biosens. Bioelectron. 212 (2022) 114412, https://doi.org/10.1016/j.bios.2022.114412.
[91] Y.C. Yang, Y.T. Lin, J. Yu, H.T. Chang, T.Y. Lu, T.Y. Huang, A. Preet, Y.J. Hsu, L. Wang, T.E. Lin, MXene nanosheet-based microneedles for monitoring muscle contraction and electrostimulation treatment, ACS Appl. Nano Mater. 4 (8) (2021) 7917, https://doi.org/10.1021/acsanm.1c01237.
[92] X. Li, X. Huang, J. Mo, H. Wang, Q. Huang, C. Yang, T. Zhang, H.-J. Chen, T. Hang, F. Liu, L. Jiang, Q. Wu, H. Li, N. Hu, X. Xie, X. Li, X. Huang, J. Mo, H. Wang, Q. Huang, C. Yang, T. Zhang, H. Chen, T. Hang, F. Liu, Q. Wu, H. Li, N. Hu, X. Xie, A fully integrated closed-loop system based on mesoporous microneedles-iontophoresis for diabetes treatment, Adv. Sci. 8 (16) (2021) 2100827, https://doi.org/10.1002/ADVS.202100827.
[93] F. Tehrani, H. Teymourian, B. Wuerstle, J. Kavner, R. Patel, A. Furmidge, R. Aghavali, H. Hosseini-Toudeshki, C. Brown, F. Zhang, K. Mahato, Z. Li, A. Barfidokht, L. Yin, P. Warren, N. Huang, Z. Patel, P.P. Mercier, J. Wang, An integrated wearable microneedle array for the continuous monitoring of multiple biomarkers in interstitial fluid, Nat. Biomed. Eng. 6 (2022) 1214, https://doi.org/10.1038/s41551-022-00887-1.
[94] K.J. Lee, S.S. Jeong, D.H. Roh, D.Y. Kim, H.-K. Choi, E.H. Lee, A practical guide to the development of microneedle systems – in clinical trials or on the market, Int. J. Pharm. 573 (2020) 118778, https://doi.org/10.1016/j.ijpharm.2019.118778.
[95] D. Kulkarni, D. Gadade, N. Chapaitkar, S. Shelke, S. Pekamwar, R. Aher, A. Ahire, M. Avhale, R. Badgule, R. Bansode, B. Bobade, Polymeric microneedles: an emerging paradigm for advanced biomedical applications, Sci. Pharm. 91 (2023) 27, https://doi.org/10.3390/scipharm91020027.
[96] M.J. Uddin, N. Scoutaris, S.N. Economidou, C. Giraud, B.Z. Chowdhry, R.F. Donnelly, D. Douroumis, 3D printed microneedles for anticancer therapy of skin tumours, Mater. Sci. Eng. C 107 (2020) 110248, https://doi.org/10.1016/j.msec.2019.110248.
[97] S.N. Economidou, C.P.P. Pere, A. Reid, MdJ. Uddin, J.F.C. Windmill, D.A. Lamprou, D. Douroumis, 3D printed microneedle patches using stereolithography (SLA) for intradermal insulin delivery, Mater. Sci. Eng. C 102 (2019) 743, https://doi.org/10.1016/j.msec.2019.04.063.
[98] A. Keirouz, Y.L. Mustafa, J.G. Turner, E. Lay, U. Jungwirth, F. Marken, H.S. Leese, Conductive polymer-coated 3D printed microneedles: biocompatible platforms for minimally invasive biosensing interfaces, Small 19 (14) (2023) 2206301, https://doi.org/10.1002/smll.202206301.
[99] L. Dai, C.L. Si, Cellulose-graft-poly(methyl methacrylate) nanoparticles with high biocompatibility for hydrophobic anti-cancer drug delivery, Mater. Lett. 207 (2017) 213, https://doi.org/10.1016/j.matlet.2017.07.090.
[100] M. Allasia, A.S. Sonzogni, V.A. Vaillard, S.E. Vaillard, L.M. Gugliotta, R.J. Minari, Methacrylated zein as a novel biobased macro-crosslinker for PVCL hydrogels, Polymer 235 (2021) 124278, https://doi.org/10.1016/j.polymer.2021.124278.
[101] B.S. Spearman, N.K. Agrawal, A. Rubiano, C.S. Simmons, S. Mobini, C.E. Schmidt, Tunable methacrylated hyaluronic acid-based hydrogels as scaffolds for soft tissue engineering applications, J. Biomed. Mater. Res. 108 (2020) 279, https://doi.org/10.1002/jbm.a.36814.
[102] H. Kumar, K. Sakthivel, M.G.A. Mohamed, E. Boras, S.R. Shin, K. Kim, Designing gelatin methacryloyl (GelMA)-Based bioinks for visible light stereolithographic 3D biofabrication, Macromol. Biosci. 21 (1) (2021) 2000317, https://doi.org/10.1002/mabi.202000317.
[103] T.O. Machado, C.J. Stubbs, V. Chiaradia, M.A. Alraddadi, A. Brandolese, J.C. Worch, A.P. Dove, A renewably sourced, circular photopolymer resin for additive manufacturing, Nature 629 (2024) 1069, https://doi.org/10.1038/s41586-024-07399-9.
[104] L. Soullard, P.A. Bayle, C. Lancelon-Pin, S. Rolere, I. Texier, B. Jean, G. Nonglaton, Optimization of the methacrylation of carboxymethylcellulose and use for the design of hydrogels and cryogels with controlled structure and properties, Cellulose 30 (2023) 6203, https://doi.org/10.1007/s10570-023-05266-w.
[105] L. Soullard, F. Pradalié, B. Labat, C. Lancelon-Pin, G. Nonglaton, S. Rolere, I. Texier, B. Jean, Methacrylated cellulose nanocrystals as fillers for the development of photo-cross-linkable cytocompatible biosourced formulations targeting 3D printing, Biomacromolecules 24 (2023) 6009, https://doi.org/10.1021/acs.biomac.3c01090.
[106] C. Li, Z. Zheng, J. Jia, W. Zhang, L. Qin, W. Zhang, Y. Lai, Preparation and characterization of photocurable composite extracellular matrix-methacrylated hyaluronic acid bioink, J. Mater. Chem. B 10 (2022) 4242, https://doi.org/10.1039/D2TB00548D.
[107] P.T. Smith, B. Narupai, S.C. Millik, R.T. Shafranek, A. Nelson, Development of bovine serum albumin-based resins for additive manufacturing via vat photopolymerization, in: E.M. Panning, M.I. Sanchez (Eds.), Novel Patterning Technologies for Semiconductors, MEMS/NEMS and MOEMS 2020, SPIE, 2020, p. 27, https://doi.org/10.1117/12.2551988.
[108] M. Zanon, R. Cue-López, E. Martínez-Campos, P. Bosch, D.-L. Versace, H. Hayek, N. Garino, C.F. Pirri, M. Sangermano, A. Chiappone, Bioderived dyes-mediated vat photopolymerization 3D printing of chitosan hydrogels for tissue engineering, Addit. Manuf. 69 (2023) 103553, https://doi.org/10.1016/j.addma.2023.103553.
[109] A.R. Parikh, K.P. Cortés-Guzmán, N. Bian, R.M. Johnson, R.A. Smaldone, H. Lu, W.E. Voit, Surface-methacrylated microcrystalline cellulose bioresins with soybean oil for additive manufacturing via vat photopolymerization, J. Polym. Sci. 62 (12) (2024) 2692, https://doi.org/10.1002/pol.20230700.
[110] S. Gopi, P. Balakrishnan, D. Chandradhara, D. Poovathankandy, S. Thomas, General scenarios of cellulose and its use in the biomedical field, Mater. Today Chem. 13 (2019) 59, https://doi.org/10.1016/j.mtchem.2019.04.012.
[111] L. Spagnuolo, R. D'Orsi, A. Operamolla, Nanocellulose for paper and textile coating: the importance of surface chemistry, Chempluschem 87 (8) (2022) e202200204, https://doi.org/10.1002/cplu.202200204.
[112] A.L. Missio, B.D. Mattos, D. de F. Ferreira, W.L.E. Magalhães, D.A. Bertuol, D.A. Gatto, A. Petutschnigg, G. Tondi, Nanocellulose-tannin films: from trees to

sustainable active packaging, J. Clean. Prod. 184 (2018) 143, https://doi.org/10.1016/j.jclepro.2018.02.205.
[113] K.B.R. Teodoro, R.C. Sanfelice, F.L. Migliorini, A. Pavinatto, M.H.M. Facure, D.S. Correa, A review on the role and performance of cellulose nanomaterials in sensors, ACS Sens. 6 (2021) 2473, https://doi.org/10.1021/acssensors.1c00473.
[114] E.J. Foster, R.J. Moon, U.P. Agarwal, M.J. Bortner, J. Bras, S. Camarero-Espinosa, K.J. Chan, M.J.D. Clift, E.D. Cranston, S.J. Eichhorn, D.M. Fox, W.Y. Hamad, L. Heux, B. Jean, M. Korey, W. Nieh, K.J. Ong, M.S. Reid, S. Renneckar, R. Roberts, J.A. Shatkin, J. Simonsen, K. Stinson-Bagby, N. Wanasekara, J. Youngblood, Current characterization methods for cellulose nanomaterials, Chem. Soc. Rev. 47 (2018) 2609, https://doi.org/10.1039/c6cs00895j.
[115] A. Amalraj, S. Gopi, S. Thomas, J.T. Haponiuk, Cellulose nanomaterials in biomedical, food, and nutraceutical applications: a review, Macromol. Symp. 380 (1) (2018) 18001151–18001159, https://doi.org/10.1002/masy.201800115.
[116] J.K. Patra, G. Das, L.F. Fraceto, E.V.R. Campos, M.D.P. Rodriguez-Torres, L.S. Acosta-Torres, L.A. Diaz-Torres, R. Grillo, M.K. Swamy, S. Sharma, S. Habtemariam, H.S. Shin, Nano based drug delivery systems: recent developments and future prospects, J Nanobiotechnol 16 (2018) 71, https://doi.org/10.1186/s12951-018-0392-8.
[117] R. Li, Y. Liu, F. Seidi, C. Deng, F. Liang, H. Xiao, Design and construction of fluorescent cellulose nanocrystals for biomedical applications, Adv. Mater. Interfac. 9 (11) (2022) 2101293, https://doi.org/10.1002/admi.202101293.
[118] M.L. Desai, S. Jha, H. Basu, S. Saha, R.K. Singhal, S.K. Kailasa, Simple hydrothermal approach for synthesis of fluorescent molybdenum disulfide quantum dots: sensing of Cr3+ ion and cellular imaging, Mater. Sci. Eng. C 111 (2020) 110778, https://doi.org/10.1016/j.msec.2020.110778.
[119] J. Wang, M. Windbergs, Functional electrospun fibers for the treatment of human skin wounds, Eur. J. Pharm. Biopharm. 119 (2017) 283, https://doi.org/10.1016/j.ejpb.2017.07.001.
[120] A. Sikder, A. Chaudhuri, S. Mondal, N.D.P. Singh, Recent advances on stimuli-responsive combination therapy against multidrug-resistant bacteria and biofilm, ACS Appl. Bio Mater. 4 (6) (2021) 4667, https://doi.org/10.1021/acsabm.1c00150.
[121] K.B.R. Teodoro, D.M. Santos, C.A.S. Ballesteros, P.A.M. Chagas, V.P. V Costa, R. Schneider, D.S. Correa, Multifunctional wound dressings based on electrospun nanofibers, in: Electrospun Nanofibers, Springer International Publishing, Cham, 2022, pp. 297–329, https://doi.org/10.1007/978-3-030-99958-2_11.
[122] N.O. Gomes, E. Carrilho, S.A.S. Machado, L.F. Sgobbi, Bacterial cellulose-based electrochemical sensing platform: a smart material for miniaturized biosensors, Electrochim. Acta 349 (2020) 136341, https://doi.org/10.1016/j.electacta.2020.136341.
[123] V. Naresh, N. Lee, A review on biosensors and recent development of nanostructured materials-enabled biosensors, Sensors 21 (4) (2021) 1109, https://doi.org/10.3390/s21041109.
[124] A. Pavinatto, L.A. Mercante, M.H.M. Facure, R.B. Pena, R.C. Sanfelice, L.H.C. Mattoso, D.S. Correa, Ultrasensitive biosensor based on polyvinylpyrrolidone/chitosan/reduced graphene oxide electrospun nanofibers for 17α – ethinylestradiol electrochemical detection, Appl. Surf. Sci. 458 (2018) 431, https://doi.org/10.1016/j.apsusc.2018.07.035.
[125] M. Guvendiren, J. Molde, R.M.D. Soares, J. Kohn, Designing biomaterials for 3D printing, ACS Biomater. Sci. Eng. 2 (10) (2016) 1679, https://doi.org/10.1021/acsbiomaterials.6b00121.
[126] A. Biswas, B. Saha, H. Bora, P.V. Vaidya, K. Dixit, S. Dhara, Introduction of 3D printing and different bioprinting methods, in: P. S.T.J.K.M.G. Saha (Ed.), 3D Bioprinting from Lab to Industry, first ed., Jonh Wiley & Sons, Inc, 2024, pp. 1–37, https://doi.org/10.1002/9781119894407.ch1.
[127] C. Oliveira, J.A. Teixeira, N. Oliveira, S. Ferreira, C.M. Botelho, Microneedles' device: design, fabrication, and applications, Macromol 4 (2) (2024) 320, https://doi.org/10.3390/macromol4020019.
[128] C.K. Chua, K.F. Leong, J. An, Introduction to rapid prototyping of biomaterials, in: Rapid Prototyping of Biomaterials: Techniques in Additive Manufacturing, second ed., Elsevier, 2019, pp. 1–15, https://doi.org/10.1016/B978-0-08-102663-2.00001-0.
[129] D.J. Thomas, M.A.B.M. Azmi, Z. Tehrani, 3D additive manufacture of oral and maxillofacial surgical models for preoperative planning, Int. J. Adv. Manuf. Technol. 71 (2014) 1643, https://doi.org/10.1007/s00170-013-5587-4.
[130] M. Błaszczyk, R. Jabbar, B. Szmyd, M. Radek, 3D printing of rapid, low-cost and patient-specific models of brain vasculature for use in preoperative planning in clipping of intracranial aneurysms, J. Clin. Med. 10 (6) (2021) 1201, https://doi.org/10.3390/jcm10061201.
[131] I. Stroud, P.C. Xirouchakis, STL and extensions, Adv. Eng. Software 31 (2000) 83, https://doi.org/10.1016/S0965-9978(99)00046-0.
[132] Z.F. Rad, P.D. Prewett, G.J. Davies, An overview of microneedle applications, materials, and fabrication methods, Beilstein J. Nanotechnol. 12 (2021) 1034, https://doi.org/10.3762/bjnano.12.77.
[133] J.M. Loh, Y.J.L. Lim, J.T. Tay, H.M. Cheng, H.L. Tey, K. Liang, Design and fabrication of customizable microneedles enabled by 3D printing for biomedical applications, Bioact. Mater. 32 (2024) 222, https://doi.org/10.1016/j.bioactmat.2023.09.022.
[134] M. Golvaskar, S.A. Ojo, M. Kannan, Recent advancements in material waste recycling: conventional, direct conversion, and additive manufacturing techniques, Recycling 9 (3) (2024) 43, https://doi.org/10.3390/recycling9030043.
[135] V. Shanmugam, O. Das, R.E. Neisiany, K. Babu, S. Singh, M.S. Hedenqvist, F. Berto, S. Ramakrishna, V. Shanmugam, O. Das, R.E. Neisiany, K. Babu, S. Singh, M.S. Hedenqvist, F. Berto, S. Ramakrishna, Polymer Recycling in Additive Manufacturing, Polymer recycling in additive manufacturing: an opportunity for the circular economy, Mater Circ Econ 2 (2020) 11, https://doi.org/10.1007/s42824-020-00012-0.
[136] S.P. Tadi, S.S. Maddula, R.S. Mamilla, Sustainability aspects of composite filament fabrication for 3D printing applications, Renew. Sustain. Energy Rev. 189 (2024) 113961, https://doi.org/10.1016/j.rser.2023.113961.
[137] M. Ali, Y. Yang, A. Abdoh, Y. Mohammed, Topographical characteristics of 3D printed polymeric microneedle surface and its impact on coating formulation attributes, RSC Applied Interfaces 1 (2024) 1108, https://doi.org/10.1039/D4LF00177J.
[138] U. Detamornrat, E. McAlister, A.R.J. Hutton, E. Larrañeta, R.F. Donnelly, The role of 3D printing technology in microengineering of microneedles, Small 18 (18) (2022) 21006392, https://doi.org/10.1002/smll.202106392.
[139] A.R. Johnson, A.T. Procopio, Low cost additive manufacturing of microneedle masters, 3D Print Med 5 (2019) 2, https://doi.org/10.1186/s41205-019-0039-x.
[140] Q. Yang, W. Zhong, L. Xu, H. Li, Q. Yan, Y. She, G. Yang, Recent progress of 3D-printed microneedles for transdermal drug delivery, Int. J. Pharm. 593 (2021) 120106, https://doi.org/10.1016/j.ijpharm.2020.120106.
[141] X. Luo, L. Yang, Y. Cui, Microneedles: materials, fabrication, and biomedical applications,, Biomed. Microdevices 25 (2023) 20, https://doi.org/10.1007/s10544-023-00658-y.
[142] M. Sirbubalo, A. Tucak, K. Muhamedagic, L. Hindija, O. Rahić, J. Hadžiabdić, A. Cekic, D. Begic-Hajdarevic, M.C. Husic, A. Dervišević, E. Vranić, 3D printing—a "touch-button" approach to manufacture microneedles for transdermal drug delivery, Pharmaceutics 13 (7) (2021) 924, https://doi.org/10.3390/pharmaceutics13070924.
[143] D. Chekkaramkodi, L. Jacob, M.S. C, R. Umer, H. Butt, Review of vat photopolymerization 3D printing of photonic devices, Addit. Manuf. 86 (2024) 104189, https://doi.org/10.1016/j.addma.2024.104189.
[144] F.M. Mwema, E.T. Akinlabi, Basics of fused deposition modelling (FDM), in: SpringerBriefs in Applied Sciences and Technology, 2020, pp. 1–15, https://doi.org/10.1007/978-3-030-48259-6_1.
[145] D. Acierno, A. Patti, Fused deposition modelling (FDM) of thermoplastic-based filaments: process and rheological properties—an overview, Materials 16 (24) (2023) 7664, https://doi.org/10.3390/ma16247664.
[146] R.B. Kristiawan, F. Imaduddin, D. Ariawan, Ubaidillah, Z. Arifin, A review on the fused deposition modeling (FDM) 3D printing: filament processing, materials, and printing parameters, Open Eng. 11 (2021) 639, https://doi.org/10.1515/eng-2021-0063.
[147] V. Mazzanti, L. Malagutti, F. Mollica, FDM 3D printing of polymers containing natural fillers: a review of their mechanical properties, Polymers 11 (7) (2019) 1094, https://doi.org/10.3390/polym11071094.
[148] A. Yadav, P. Rohru, A. Babbar, R. Kumar, N. Ranjan, J.S. Chohan, R. Kumar, M. Gupta, Fused filament fabrication: a state-of-the-art review of the technology, materials, properties and defects, Int. J. Interact. Des. Manuf. 17 (2023) 2867, https://doi.org/10.1007/s12008-022-01026-5.
[149] V.M. Bruère, A. Lion, J. Holtmannspötter, M. Johlitz, The influence of printing parameters on the mechanical properties of 3D printed TPU-based elastomers, Progress in Additive Manufacturing 8 (2023) 693, https://doi.org/10.1007/s40964-023-00418-7.
[150] L. Großmann, M. Kieckhöfer, W. Weitschies, J. Krause, 4D prints of flexible dosage forms using thermoplastic polyurethane with hybrid shape memory effect, Eur. J. Pharm. Biopharm. 181 (2022) 227, https://doi.org/10.1016/j.ejpb.2022.11.009.
[151] B.G. Thiam, A. El Magri, S. Vaudreuil, Cost estimation and performance evaluation of 3D printed membranes for vanadium redox flow batteries, Energy Storage 6 (1) (2024) e536, https://doi.org/10.1002/est2.536.
[152] P. Bettini, G. Alitta, G. Sala, L. Di Landro, Fused deposition technique for continuous fiber reinforced thermoplastic, J. Mater. Eng. Perform. 26 (2017) 843, https://doi.org/10.1007/s11665-016-2459-8.
[153] G. Gonzalez, I. Roppolo, C.F. Pirri, A. Chiappone, Current and emerging trends in polymeric 3D printed microfluidic devices, Addit. Manuf. 55 (2022) 102867, https://doi.org/10.1016/j.addma.2022.102867.
[154] N. Vidakis, M. Petousis, E. Velidakis, N. Mountakis, P.E. Fischer-Griffiths, S. Grammatikos, L. Tzounis, Fused filament fabrication three-dimensional printing multi-functional of polylactic acid/carbon black nanocomposites, Journal of Carbon Research 7 (2021) 52, https://doi.org/10.3390/c7030052.
[155] S. Giner-Grau, C. Lazaro-Hdez, J. Pascual, O. Fenollar, T. Boronat, Enhancing polylactic acid properties with graphene nanoplatelets and carbon black nanoparticles: a study of the electrical and mechanical characterization of 3D-printed and injection-molded samples, Polymers 16 (2024) 2449, https://doi.org/10.3390/polym16172449.
[156] E. Ivanov, R. Kotsilkova, H. Xia, Y. Chen, R.K. Donato, K. Donato, A.P. Godoy, R. Di Maio, C. Silvestre, S. Cimmino, V. Angelov, PLA/Graphene/MWCNT composites with improved electrical and thermal properties suitable for FDM 3D printing applications, Appl. Sci. 9 (2019) 1209, https://doi.org/10.3390/app9061209.
[157] H.K. Sezer, O. Eren, FDM 3D printing of MWCNT re-inforced ABS nano-composite parts with enhanced mechanical and electrical properties, J. Manuf. Process. 37 (2019) 339, https://doi.org/10.1016/j.jmapro.2018.12.004.
[158] R.D. Crapnell, I.V.S. Arantes, J.R. Camargo, E. Bernalte, M.J. Whittingham, B.C. Janegitz, T.R.L.C. Paixão, C.E. Banks, Multi-walled carbon nanotubes/carbon black/rPLA for high-performance conductive additive manufacturing filament and the simultaneous detection of acetaminophen and phenylephrine, Microchim. Acta 191 (2024) 96, https://doi.org/10.1007/s00604-023-06175-2.
[159] M.C. Kouassi, A. Ben Abdallah, S. Nouira, S. Ballut, J. Fitoussi, M. Shirinbayan, A. Kallel, FDM printing of microneedles based on biocompatible and

biodegradable thermoplastic polymers, J. Appl. Polym. Sci. 141 (2024) e56067, https://doi.org/10.1002/app.56067.
[160] L. Wu, J. Park, Y. Kamaki, B. Kim, Optimization of the fused deposition modeling-based fabrication process for polylactic acid microneedles, Microsyst Nanoeng 7 (2021) 58, https://doi.org/10.1038/s41378-021-00284-9.
[161] A. Khosraviboroujeni, S.Z. Mirdamadian, M. Minaiyan, A. Taheri, Preparation and characterization of 3D printed PLA microneedle arrays for prolonged transdermal drug delivery of estradiol valerate, Drug Deliv Transl Res 12 (2022) 1195, https://doi.org/10.1007/s13346-021-01006-4.
[162] M. Lebedevaite, V. Talacka, J. Ostrauskaite, High biorenewable content acrylate photocurable resins for DLP 3D printing, J. Appl. Polym. Sci. 138 (2021) e50233, https://doi.org/10.1002/app.50233.
[163] S.C. Tsai, L.H. Chen, C.P. Chu, W.C. Chao, Y.C. Liao, Photo curable resin for 3D printed conductive structures, Addit. Manuf. 51 (2022) 102590, https://doi.org/10.1016/j.addma.2021.102590.
[164] A.J. Guerra, J. Lammel-Lindemann, A. Katko, A. Kleinfehn, C.A. Rodriguez, L.H. Catalani, M.L. Becker, J. Ciurana, D. Dean, Optimization of photocrosslinkable resin components and 3D printing process parameters, Acta Biomater. 97 (2019) 154, https://doi.org/10.1016/j.actbio.2019.07.045.
[165] A.J. Guerra, H. Lara-Padilla, M.L. Becker, C.A. Rodriguez, D. Dean, Photopolymerizable resins for 3D-printing solid-cured tissue engineered implants, Curr. Drug Targets 20 (2019) 823, https://doi.org/10.2174/1389450120666190114122815.
[166] H. Erkus, T. Bedir, E. Kaya, G.B. Tinaz, O. Gunduz, M.C. Chifiriuc, C.B. Ustundag, Innovative transdermal drug delivery system based on amoxicillin-loaded gelatin methacryloyl microneedles obtained by 3D printing, Materialia (Oxf) 27 (2023) 101700, https://doi.org/10.1016/j.mtla.2023.101700.
[167] S. Dey, C. Jaiswal, S. Shome, B. Bhar, A. Bandyopadhyay, K. Manikumar, R. Dadheech, B.B. Mandal, Photocrosslinkable silk-based biomaterials for regenerative medicine and healthcare applications, Regen Eng Transl Med 9 (2022) 181, https://doi.org/10.1007/s40883-022-00277-8.
[168] M.B. Sharma, H.A.M. Abdelmohsen, Ö. Kap, V. Kilic, N. Horzum, D. Cheneler, J.G. Hardy, Poly(2-Hydroxyethyl methacrylate) hydrogel-based microneedles for bioactive release, Bioengineering 11 (7) (2024) 649, https://doi.org/10.3390/bioengineering11070649.
[169] L. Soullard, A. Schlepp, R. Buret, C. Lancelon-Pin, G. Nonglaton, I. Texier, B. Jean, S. Rolere, Towards the 3D printing of innovative hydrogel scaffolds through vat polymerization techniques using methacrylated carboxymethylcellulose aqueous formulations, Progress in Additive Manufacturing (2024) 0123456789, https://doi.org/10.1007/s40964-024-00744-4.
[170] Q.T. Che, J.W. Seo, K. Charoensri, M.H. Nguyen, H.J. Park, H. Bae, 4D-printed microneedles from dual-sensitive chitosan for non-transdermal drug delivery, Int. J. Biol. Macromol. 261 (2024) 129638, https://doi.org/10.1016/j.ijbiomac.2024.129638.
[171] S.H. Park, Y.J. Kim, S. Park, H. Hong, J.Y. Lee, S. Il Kim, K.J. Lee, W.H. Ryu, Rapid extraction and detection of biomolecules via a microneedle array of wet-crosslinked methacrylated hyaluronic acid, Adv Mater Technol 7 (3) (2022) 2100874, https://doi.org/10.1002/admt.202100874.
[172] J. Chudzińska, A. Wawrzyńczak, A. Feliczak-Guzik, Microneedles based on a biodegradable polymer—hyaluronic acid, Polymers 16 (10) (2024) 1396, https://doi.org/10.3390/polym16101396.
[173] A. Bagheri, J. Jin, Photopolymerization in 3D printing, ACS Appl. Polym. Mater. 1 (4) (2019) 593, https://doi.org/10.1021/acsapm.8b00165.
[174] J. Zhang, P. Xiao, 3D printing of photopolymers, Polym. Chem. 9 (2018) 1530, https://doi.org/10.1039/c8py00157j.
[175] Y. Bao, Recent trends in advanced photoinitiators for vat photopolymerization 3D printing, Macromol. Rapid Commun. 43 (2022) 2200202, https://doi.org/10.1002/marc.202200202.
[176] K. Sun, X. Peng, Z. Gan, W. Chen, X. Li, T. Gong, P. Xiao, 3D printing/vat photopo lymerization of photopolymers activated by novel organic dyes as photoinitiators, Catalysts 12 (10) (2022) 1272, https://doi.org/10.3390/catal12101272.
[177] P. Fiedor, M. Pilch, P. Szymaszek, A. Chachaj-Brekiesz, M. Galek, J. Ortyl, Photochemical study of a new bimolecular photoinitiating system for vat photopolymerization 3D printing techniques under visible light, Catalysts 10 (3) (2020) 284, https://doi.org/10.3390/catal10030284.
[178] L. Breloy, V. Brezová, Z. Barbieriková, Y. Ito, J. Akimoto, A. Chiappone, S. Abbad-Andaloussi, J.P. Malval, D.L. Versace, Methacrylated quinizarin derivatives for visible-light mediated photopolymerization: promising applications in 3D-printing biosourced materials under LED@405 nm, ACS Appl. Polym. Mater. 4 (1) (2022) 210, https://doi.org/10.1021/acsapm.1c01210.
[179] M. Jankowska, A. Chachaj-Brekiesz, K. Trembecka-Wójciga, A. Jarzębska, M. Topa-Skwarczyńska, M. Pilch, J. Ortyl, Novel multi-material photo-curable resins containing high-performance photoinitiating systems and nano additives dedicated to 3D-VAT printing, Polym. Chem. 14 (2023) 2088, https://doi.org/10.1039/d2py01583h.
[180] H. Quan, T. Zhang, H. Xu, S. Luo, J. Nie, X. Zhu, Bioactive Materials Photo-curing 3D printing technique and its challenges, Bioact. Mater. 5 (2020) 110, https://doi.org/10.1016/j.bioactmat.2019.12.003.
[181] F. Trends, M. Pagac, J. Hajnys, Q. Ma, L. Jancar, J. Jansa, P. Stefek, J. Mesicek, A review of vat photopolymerization technology: materials, applications, challenges, and future trends of 3D printing, Polymers 13 (4) (2021) 598, https://doi.org/10.3390/polym13040598.
[182] R. Liang, Y. Gu, Y. Wu, V. Bunpetch, S. Zhang, Lithography-based 3D bioprinting and bioinks for bone repair and regeneration, ACS Biomater. Sci. Eng. 7 (3) (2021) 806, https://doi.org/10.1021/acsbiomaterials.9b01818.
[183] A. Al Rashid, W. Ahmed, M.Y. Khalid, M. Koç, Vat photopolymerization of polymers and polymer composites: processes and applications, Addit. Manuf. 47 (2021) 102279, https://doi.org/10.1016/j.addma.2021.102279.
[184] Y. Li, W. Wang, F. Wu, R.K. Kankala, Vat polymerization-based 3D printing of nanocomposites: a mini review, Front Mater 9 (2023) 1, https://doi.org/10.3389/fmats.2022.1118943.
[185] S. Ligati Schleifer, O. Sheinfeld, O. Regev, Vat photopolymerization of polymer composites with printing-direction-independent properties, Addit. Manuf. 92 (2024) 104372, https://doi.org/10.1016/j.addma.2024.104372.
[186] P. Gruhn, D. Koske, J.L. Storck, A. Ehrmann, Three-dimensional printing by vat photopolymerization on textile fabrics: method and mechanical properties of the textile/polymer composites, Textiles 4 (2024) 417, https://doi.org/10.3390/textiles4030024.
[187] M. Shah, A. Ullah, K. Azher, A.U. Rehman, W. Juan, N. Aktürk, C.S. Tüfekci, M.U. Salamci, Vat photopolymerization-based 3D printing of polymer nanocomposites: current trends and applications, RSC Adv. 13 (2023) 1456, https://doi.org/10.1039/d2ra06522c.
[188] W. Wang, J. Sun, B. Guo, X. Chen, K.P. Ananth, J. Bai, Fabrication of piezoelectric nano-ceramics via stereolithography of low viscous and non-aqueous suspensions, J. Eur. Ceram. Soc. 40 (2020) 682, https://doi.org/10.1016/j.jeurceramsoc.2019.10.033.
[189] S.S. Ray, H. Dommati, J.C. Wang, S.S. Chen, Solvent based Slurry Stereolithography 3D printed hydrophilic ceramic membrane for ultrafiltration application, Ceram. Int. 46 (2020) 12480, https://doi.org/10.1016/j.ceramint.2020.02.010.
[190] S.D. Silbert, P. Simpson, R. Setien, M. Holthaus, J. La Scala, C.A. Ulven, D.C. Webster, Exploration of bio-based functionalized sucrose ester resins for additive manufacturing via stereolithography, ACS Appl. Polym. Mater. 2 (2020) 2910, https://doi.org/10.1021/acsapm.0c00417.
[191] D.N. Heo, S.J. Lee, R. Timsina, X. Qiu, N.J. Castro, L.G. Zhang, Development of 3D printable conductive hydrogel with crystallized PEDOT:PSS for neural tissue engineering, Mater. Sci. Eng. C 99 (2019) 582, https://doi.org/10.1016/j.msec.2019.02.008.
[192] W. Duan, S. Li, G. Wang, R. Dou, L. Wang, Y. Zhang, H. Li, H. Tan, Thermal conductivities and mechanical properties of AlN ceramics fabricated by three dimensional printing, J. Eur. Ceram. Soc. 40 (2020) 3535, https://doi.org/10.1016/j.jeurceramsoc.2020.04.004.
[193] I. Xenikakis, K. Tsongas, E.K. Tzimtzimis, C.K. Zacharis, N. Theodoroula, E.P. Kalogianni, E. Demiri, I.S. Vizirianakis, D. Tzetzis, D.G. Fatouros, Fabrication of hollow microneedles using liquid crystal display (LCD) vat polymerization 3D printing technology for transdermal macromolecular delivery, Int. J. Pharm. 597 (2021) 120303, https://doi.org/10.1016/j.ijpharm.2021.120303.
[194] M.G.A. Mohamed, H. Kumar, Z. Wang, N. Martin, B. Mills, K. Kim, Rapid and inexpensive fabrication of multi-depth microfluidic device using high-resolution LCD stereolithographic 3D printing, Journal of Manufacturing and Materials Processing 3 (1) (2019) 26, https://doi.org/10.3390/jmmp3010026.
[195] E.F. dos Santos, L.G. Maciel, J.H. Araujo-Neto, D.K.D. Nascimento, W. Barros-Junior, J.V. dos Anjos, S. Alves-Junior, A novel and biocompatible photopolymerizable resin based on cyclohexanedimethanol-dimetacrylate designed to light-print microneedles, J. Appl. Polym. Sci. 141 (2024) e55736, https://doi.org/10.1002/app.55736.
[196] I. Xenikakis, K. Tsongas, E.K. Tzimtzimis, O.L. Katsamenis, E. Demiri, C.K. Zacharis, D. Georgiou, E.P. Kalogianni, D. Tzetzis, D.G. Fatouros, Transdermal delivery of insulin across human skin in vitro with 3D printed hollow microneedles, J. Drug Deliv. Sci. Technol. 67 (2022) 102891, https://doi.org/10.1016/j.jddst.2021.102891.
[197] B. Chanabodeechalermrung, T. Chaiwarit, S. Chaichit, S. Udomsom, P. Baipaywad, P. Worajittiphon, P. Jantrawut, HPMC/PVP K90 dissolving microneedles fabricated from 3D-printed master molds: impact on microneedle morphology, mechanical strength, and topical dissolving property, Polymers 16 (2024) 452, https://doi.org/10.3390/polym16040452.
[198] I. Xenikakis, K. Tsongas, E.K. Tzimtzimis, D. Tzetzis, D. Fatouros, Additive manufacturing of hollow microneedles for insulin delivery, International Journal of Modern Manufacturing Technologies 13 (2021) 185, https://doi.org/10.54684/ijmmt.2021.13.3.185.
[199] R.V. Pazhamannil, P. Govindan, Current state and future scope of additive manufacturing technologies via vat photopolymerization, Mater. Today Proc. 43 (2020) 130, https://doi.org/10.1016/j.matpr.2020.11.225.
[200] J.R. Tumbleston, D. Shirvanyants, N. Ermoshkin, R. Janusziewicz, A.R. Johnson, D. Kelly, K. Chen, R. Pinschmidt, J.P. Rolland, A. Ermoshkin, E.T. Samulski, J.M. DeSimone, Continuous liquid interface production of3D objects, Sci. Adv. 347 (2015) 1349, https://doi.org/10.1126/sciadv.abq3917.
[201] D.E. Düzgün, K. Nadolny, Continuous liquid interface production (CLIP) method for rapid prototyping, Journal of Mechanical and Energy Engineering 2 (2018) 5, https://doi.org/10.30464/jmee.2018.2.1.5.
[202] R. Janusziewicz, J.R. Tumbleston, A.L. Quintanilla, S.J. Mecham, J.M. DeSimone, Layerless fabrication with continuous liquid interface production, Proc. Natl. Acad. Sci. U. S. A. 113 (2016) 11703, https://doi.org/10.1073/pnas.1605271113.
[203] K. Hsiao, B.J. Lee, T. Samuelsen, G. Lipkowitz, J.M. Kronenfeld, D. Ilyn, A. Shih, M.T. Dulay, L. Tate, E.S.G. Shaqfeh, J.M. DeSimone, Single-digit-micrometer-resolution continuous liquid interface production, Sci. Adv. 8 (2022), https://doi.org/10.1126/sciadv.abq2846 eabq2846.
[204] A.R. Johnson, C.L. Caudill, J.R. Tumbleston, C.J. Bloomquist, K.A. Moga, A. Ermoshkin, D. Shirvanyants, S.J. Mecham, J.C. Luft, J.M. DeSimone, Single-step fabrication of computationally designed microneedles by continuous liquid

interface production, PLoS One 11 (2016) e0162518, https://doi.org/10.1371/journal.pone.0162518.
[205] N.U. Rajesh, J. Hwang, Y. Xu, M.A. Saccone, A.H. Hung, R.A.S. Hernandez, I.A. Coates, M.M. Driskill, M.T. Dulay, G.B. Jacobson, S. Tian, J.L. Perry, J.M. DeSimone, 3D-Printed latticed microneedle array patches for tunable and versatile intradermal delivery, Advanced Materials 36 (44) (2024) 24046061, https://doi.org/10.1002/adma.202404606.
[206] S. Kawre, P. Suryavanshi, D.S. Lalchandani, M.K. Deka, P. Kumar, S. Kaity, S. Roy, S. Banerjee, Bioinspired labrum-shaped stereolithography (SLA) assisted 3D printed hollow microneedles (HMNs) for effectual delivery of ceftriaxone sodium, Eur. Polym. J. 204 (2024) 112702, https://doi.org/10.1016/j.eurpolymj.2023.112702.
[207] M.J. Uddin, N. Scoutaris, S.N. Economidou, C. Giraud, B.Z. Chowdhry, R.F. Donnelly, D. Douroumis, 3D printed microneedles for anticancer therapy of skin tumours, Mater. Sci. Eng. C 107 (2020) 110248, https://doi.org/10.1016/j.msec.2019.110248.
[208] L. Santra, W.J. Furiosi, A. Kundu, S. Rajaraman, A Minimally-Invasive 3D-Printed Microneedle Array Applicator System (μNAAS) for Delivery of Therapeutics to Citrus Leaf Tissue, J. Young Investigators 39 (5) (2021) 60.
[209] R. Palucci Rosa, G. Rosace, Nanomaterials for 3D printing of polymers via stereolithography: concept, technologies, and applications, Macromol. Mater. Eng. 306 (10) (2021) 2100345, https://doi.org/10.1002/mame.202100345.
[210] R.J. Mondschein, A. Kanitkar, C.B. Williams, S.S. Verbridge, T.E. Long, Polymer structure-property requirements for stereolithographic 3D printing of soft tissue engineering scaffolds, Biomaterials 140 (2017) 170, https://doi.org/10.1016/j.biomaterials.2017.06.005.
[211] Y. Pan, H. He, J. Xu, A. Feinerman, Study of separation force in constrained surface projection stereolithography, Rapid Prototyp. J. 23 (2017) 353, https://doi.org/10.1108/RPJ-12-2015-0188.
[212] J. Gong, Y. Qian, K. Lu, Z. Zhu, L. Siow, C. Zhang, S. Zhou, Digital light processing (DLP) in tissue engineering: from promise to reality, and perspectives, Biomed. Mater. 17 (6) (2022) 062004, https://doi.org/10.1088/1748-605X/ac96ba.
[213] S. Swetha, T.J. Sahiti, G.S. Priya, K. Harshitha, A. Anil, Review on digital light processing (DLP) and effect of printing parameters on quality of print, Interactions 245 (2024) 178, https://doi.org/10.1007/s10751-024-02018-5.
[214] E. Mathew, G. Pitzanti, A.L. Gomes, D.A. Lamprou, Optimization of printing parameters for digital light processing 3D printing of hollow microneedle arrays, Pharmaceutics 13 (11) (2021) 1837, https://doi.org/10.3390/pharmaceutics13111837.
[215] D. Shin, J. Hyun, Silk fibroin microneedles fabricated by digital light processing 3D printing, J. Ind. Eng. Chem. 95 (2021) 126, https://doi.org/10.1016/j.jiec.2020.12.011.
[216] A. Kundu, P. Arnett, A. Bagde, N. Azim, E. Kouagou, M. Singh, S. Rajaraman, DLP 3D printed " intelligent " microneedle array (iμ NA) for stimuli responsive release of drugs and its in vitro and ex vivo characterization, J. Microelectromech. Syst. 29 (2020) 685, https://doi.org/10.1109/JMEMS.2020.3003628.
[217] W. Yao, D. Li, Y. Zhao, Z. Zhan, G. Jin, H. Liang, R. Yang, 3D Printed multi-functional hydrogel microneedles based on high-precision digital light processing, Micromachines 11 (1) (2020) 17, https://doi.org/10.3390/mi11010017.
[218] M. Ali, S. Namjoshi, K. Phan, X. Wu, I. Prasadam, H.A.E. Benson, T. Kumeria, Y. Mohammed, 3D printed microneedles for the transdermal delivery of NAD+ precursor: toward personalization of skin delivery, ACS Biomater. Sci. Eng. 10 (11) (2024) 7235, https://doi.org/10.1021/acsbiomaterials.4c00905.
[219] A. Bagde, K. Mosley-Kellum, S. Spencer, M. Singh, 3D DLP-printed cannabinoid microneedles patch and its pharmacokinetic evaluation in rats, J. Pharm. Pharmacol. 76 (2024) 616, https://doi.org/10.1093/jpp/rgae043.
[220] A. Bagde, S. Dev, L. Madhavi K. Sriram, S.D. Spencer, A. Kalvala, A. Nathani, O. Salau, K. Mosley-Kellum, H. Dalvaigari, S. Rajaraman, A. Kundu, M. Singh, Biphasic burst and sustained transdermal delivery in vivo using an AI-optimized 3D-printed MN patch, Int. J. Pharm. 636 (2023) 122647, https://doi.org/10.1016/j.ijpharm.2023.122647.
[221] Y. Sun, X. Wang, M. Tang, M.K. Melarkey, T. yu Lu, Y. Xiang, S. Chen, 3D printing of succulent-inspired microneedle array for enhanced tissue adhesion and controllable drug release, Adv Mater Technol 9 (15) (2024) 2400216, https://doi.org/10.1002/admt.202400216.
[222] H. Liu, X. Zhou, A. Nail, H. Yu, Z. Yu, Y. Sun, K. Wang, N. Bao, D. Meng, L. Zhu, H. Li, Multi-material 3D printed eutectogel microneedle patches integrated with fast customization and tunable drug delivery, J. Contr. Release 368 (2024) 115, https://doi.org/10.1016/j.jconrel.2024.02.023.
[223] A.G. Tabriz, B. Viegas, M. Okereke, J. Uddin, E.A. Lopez, N. Zand, M. Ranatunga, G. Getti, D. Douroumis, Evaluation of 3D printability and biocompatibility of microfluidic resin for fabrication of solid microneedles, Micromachines 13 (9) (2022) 1368. http://doi.org/10.3390/mi13091368.
[224] C. Liao, W. Anderson, F. Antaw, M. Trau, Two-photon nanolithography of tailored hollow three-dimensional microdevices for biosystems, ACS Omega 4 (2019) 1401, https://doi.org/10.1021/acsomega.8b03164.
[225] W. Cao, W. Yu, Z. Xiao, W. Xin, Y. Wu, H. Zheng, Water flow tuned by micro/nano hierarchical structures fabricated through two-photon polymerization, Materials Science in Additive Manufacturing 2 (2023) 0879, https://doi.org/10.36922/msam.0879.
[226] C. Xu, C. Zhang, W. Zhao, Y. Liu, Z. Li, Z. Wang, B. Lu, K. Wang, J. Bai, Fabrication of micro/nano dual needle structures with morphological gradient based on two-photon polymerization laser direct writing with proactive focus compensation, Photonics 11 (2024) 187, https://doi.org/10.3390/photonics11020187.
[227] S.D. Gittard, A. Ovsianikov, B.N. Chichkov, A. Doraiswamy, R.J. Narayan, Two photon polymerization of microneedles for transdermal drug delivery, Expet Opin. Drug Deliv. 7 (2010) 513, https://doi.org/10.1517/17425241003628171.Two.
[228] A.I. Ciuciu, P.J. Cywiński, Two-photon polymerization of hydrogels-versatile solutions to fabricate well-defined 3D structures, RSC Adv. 4 (2014) 45504–45516, https://doi.org/10.1039/c4ra06892k.
[229] S. O'Halloran, A. Pandit, A. Heise, A. Kellett, Two-photon polymerization: fundamentals, materials, and chemical modification strategies, Adv. Sci. 10 (2023) 2204072, https://doi.org/10.1002/advs.202204072.
[230] A. Jaiswal, C.K. Rastogi, S. Rani, G.P. Singh, S. Saxena, S. Shukla, Two decades of two-photon lithography: materials science perspective for additive manufacturing of 2D/3D nano-microstructures, iScience 26 (2023) 106374, https://doi.org/10.1016/j.isci.2023.106374.
[231] W. Wang, Z.Q. Chen, B. Lin, M.C. Liu, Y. Zhang, S.J. Liu, Y. Li, Q. Zhao, Two-photon polymerization-based 3D micro-scaffolds toward biomedical devices, Chem. Eng. J. 493 (2024) 152469, https://doi.org/10.1016/j.cej.2024.152469.
[232] X. Jing, H. Fu, B. Yu, M. Sun, L. Wang, Two-photon polymerization for 3D biomedical scaffolds: overview and updates, Front. Bioeng. Biotechnol. 10 (2022) 1, https://doi.org/10.3389/fbioe.2022.994355.
[233] S. Mckee, A. Lutey, C. Sciancalepore, F. Poli, S. Selleri, A. Cucinotta, Microfabrication of polymer microneedle arrays using two-photon polymerization, J. Photochem. Photobiol., B 229 (2022) 112424, https://doi.org/10.1016/j.jphotobiol.2022.112424.
[234] Z. He, F. Chen, S. He, Fabrication of microneedles using two photon-polymerization with low numerical aperture, Opt. Commun. 553 (2024) 130093, https://doi.org/10.1016/j.optcom.2023.130093.
[235] A.S. Cordeiro, I.A. Tekko, M.H. Jomaa, L. Vora, E. Mcalister, F. Volpe-zanutto, M. Nethery, P.T. Baine, N. Mitchell, D.W. Mcneill, F. Ryan, Two-photon polymerisation 3D printing of microneedle array templates with versatile designs: application in the development of polymeric drug delivery systems, Pharm. Res. 37 (9) (2020) 174, https://doi.org/10.1007/s11095-020-02887-9.
[236] M.M. Pillai, S. Ajesh, P. Tayalia, Two-photon polymerization based reusable master template to fabricate polymer microneedles for drug delivery, MethodsX 10 (2023) 102025, https://doi.org/10.1016/j.mex.2023.102025.
[237] C.N. LaFratta, T. Baldacchini, Two-photon polymerization metrology: characterization methods of mechanisms and microstructures, Micromachines 8 (4) (2017) 101, https://doi.org/10.3390/mi8040101.
[238] J.M. Loh, Y.J.L. Lim, J.T. Tay, H.M. Cheng, H.L. Tey, K. Liang, Design and fabrication of customizable microneedles enabled by 3D printing for biomedical applications, Bioact. Mater. 32 (2024) 222, https://doi.org/10.1016/j.bioactmat.2023.09.022.
[239] T.N. Tarbox, A.B. Watts, Z. Cui, R.O. Williams, An update on coating/manufacturing techniques of microneedles, Drug Deliv Transl Res 8 (2018) 1828, https://doi.org/10.1007/s13346-017-0466-4.
[240] H. Liu, A. Nail, D. Meng, L. Zhu, X. Guo, C. Li, H.-J. Li, Recent progress in the 3D printing of microneedle patches for biomedical applications, Int. J. Pharm. 668 (2025) 124995, https://doi.org/10.1016/j.ijpharm.2024.124995.
[241] A.A. Biswas, M.R. Dhondale, A.K. Agrawal, D.R. Serrano, B. Mishra, D. Kumar, Advancements in microneedle fabrication techniques: artificial intelligence assisted 3D-printing technology, Drug Deliv Transl Res 14 (2024) 1458–1479, https://doi.org/10.1007/s13346-023-01510-9.
[242] W. He, S. Kong, R. Lin, Y. Xie, S. Zheng, Z. Yin, X. Huang, L. Su, X. Zhang, Machine learning assists in the design and application of microneedles, Biomimetics 9 (2024) 469, https://doi.org/10.3390/biomimetics9080469.
[243] H. Haick, N. Tang, Artificial intelligence in medical sensors for clinical decisions, ACS Nano 15 (2021) 3557, https://doi.org/10.1021/acsnano.1c00085.
[244] M.R. Sarabi, M.M. Alseed, A.A. Karagoz, S. Tasoglu, Machine learning-enabled prediction of 3D-printed microneedle features, Biosensors 12 (2022) 491, https://doi.org/10.3390/bios12070491.
[245] M. Zhang, X. Guo, J. Wang, Advanced biosensors for mycotoxin detection incorporating miniaturized meters, Biosens. Bioelectron. 224 (2023) 115077, https://doi.org/10.1016/j.bios.2023.115077.
[246] X. Li, S. Zhou, Z. Deng, B. Liu, B. Gao, Corn-inspired high-density plasmonic metal-organic frameworks microneedles for enhanced SERS detection of acetaminophen, Talanta 278 (2024) 126463, https://doi.org/10.1016/j.talanta.2024.126463.
[247] I.R. Ausri, S. Sadeghzadeh, S. Biswas, H. Zheng, P. GhavamiNejad, M.D.T. Huynh, F. Keyvani, E. Shirzadi, F.A. Rahman, J. Quadrilatero, A. GhavamiNejad, M. Poudineh, Multifunctional dopamine-based hydrogel microneedle electrode for continuous ketone sensing, Adv. Mater. 36 (32) (2024) 2402009, https://doi.org/10.1002/adma.202402009.
[248] F. Luo, Z. Li, Y. Shi, W. Sun, Y. Wang, J. Sun, Z. Fan, Y. Chang, Z. Wang, Y. Han, Z. Zhu, J.L. Marty, Integration of hollow microneedle arrays with jellyfish-shaped electrochemical sensor for the detection of biomarkers in interstitial fluid, Sensors 24 (12) (2024) 3729, https://doi.org/10.3390/s24123729.
[249] Y. Wu, F. Tehrani, H. Teymourian, J. Mack, A. Shaver, M. Reynoso, J. Kavner, N. Huang, A. Furmidge, A. Duvvuri, Y. Nie, L.M. Laffel, F.J. Doyle, M.E. Patti, E. Dassau, J. Wang, N. Arroyo-Currás, Microneedle aptamer-based sensors for continuous, real-time therapeutic drug monitoring, Anal. Chem. 94 (2022) 8335, https://doi.org/10.1021/acs.analchem.2c00829.
[250] M. Parrilla, A. Vanhooydonck, M. Johns, R. Watts, K. De Wael, 3D-printed microneedle-based potentiometric sensor for pH monitoring in skin interstitial fluid, Sens Actuators B Chem 378 (2023) 133159, https://doi.org/10.1016/j.snb.2022.133159.
[251] P. Miller, M. Moorman, R. Manginell, C. Ashlee, I. Brener, D. Wheeler, R. Narayan, R. Polsky, Towards an integrated microneedle total analysis chip for protein

detection, Electroanalysis 28 (2016) 1305, https://doi.org/10.1002/elan.201600063.
[252] J. Cheng, J. Huang, Q. Xiang, H. Dong, Hollow microneedle microfluidic paper-based chip for biomolecules rapid sampling and detection in interstitial fluid, Anal. Chim. Acta 1255 (2023) 341101, https://doi.org/10.1016/j.aca.2023.341101.
[253] Y. Xie, K. Li, J. Liu, Y. Zhou, C. Zhang, Y. Yu, J. Wang, L. Su, X. Zhang, A smart lab on a wearable microneedle patch with convolutional neural network-enhanced colorimetry for early warning of syndrome of inappropriate antidiuretic hormone secretion, Aggregate 6 (6) (2024) e671, https://doi.org/10.1002/agt2.671.
[254] T.Q. Ma, Q.Y. He, X.Y. Li, B. Zhang, Y.L. Li, L.J. Chen, X.Q. You, J. Liu, Wearable microneedle sensor with replaceable sensor base for multi-purpose detecting in skin interstitial fluid, Microchem. J. 203 (2024) 110933, https://doi.org/10.1016/j.microc.2024.110933.
[255] Y. Liu, L. Yang, Y. Cui, A wearable, rapidly manufacturable, stability-enhancing microneedle patch for closed-loop diabetes management, Microsyst Nanoeng 10 (112) (2024) 1, https://doi.org/10.1038/s41378-024-00663-y.
[256] Y. Liu, Q. Yu, X. Luo, L. Yang, Y. Cui, Continuous monitoring of diabetes with an integrated microneedle biosensing device through 3D printing, Microsyst Nanoeng 7 (75) (2021), https://doi.org/10.1038/s41378-021-00302-w.
[257] M. Razzaghi, A. Seyfoori, E. Pagan, E. Askari, A. Hassani Najafabadi, M. Akbari, 3D printed hydrogel microneedle arrays for interstitial fluid biomarker extraction and colorimetric detection, Polymers 15 (6) (2023) 1389, https://doi.org/10.3390/polym15061389.
[258] T. Wu, X. You, Z. Chen, Hollow microneedles on a paper fabricated by standard photolithography for the screening test of prediabetes, Sensors 22 (11) (2022) 4253, https://doi.org/10.3390/s22114253.
[259] D. Jin, Z. Xu, H. Zhao, S. Deng, Z. Qu, R. Dou, W. Liu, A minimally invasive sensing system based on hydrogel microneedle patches and Au/Cu2O nanospheres modified screen-printed carbon electrode for glucose monitoring in interstitial skin fluid, Microchem. J. 205 (2024) 111367, https://doi.org/10.1016/j.microc.2024.111367.
[260] S. Lin, Y. Ouyang, W. Lin, X. Zhou, M. Miao, E. Cheng, Y. Jiang, Z. Meng, M. Jin, S. Zhang, S. Li, X. Lv, S. Chen, Y. Guo, J. Zhang, K. Cai, Z. Lin, F. Yang, J. Zhu, Microenvironment-optimized GelMA microneedles for interstitial fluid extraction and real-time glucose detection, Surf. Interfaces 45 (2024) 103847, https://doi.org/10.1016/j.surfin.2024.103847.
[261] Y. Pang, Y. Li, K. Chen, M. Wu, J. Zhang, Y. Sun, Y. Xu, X. Wang, Q. Wang, X. Ning, D. Kong, Porous microneedles through direct ink drawing with nanocomposite inks for transdermal collection of interstitial fluid, Small 20 (23) (2024) 2305838, https://doi.org/10.1002/smll.202305838.
[262] Y. Yin, X. Li, M. Wang, G. Ling, P. Zhang, Glucose detection: in-situ colorimetric analysis with double-layer hydrogel microneedle patch based on polyvinyl alcohol and carboxymethyl chitosan, Int. J. Biol. Macromol. 277 (2024) 134408, https://doi.org/10.1016/j.ijbiomac.2024.134408.
[263] M. Dervisevic, N.H. Voelcker, Microneedles with recessed microcavities for electrochemical sensing in dermal interstitial fluid, ACS Mater. Lett. 5 (2023) 1851, https://doi.org/10.1021/acsmaterialslett.3c00441.
[264] M. Dervisevic, M.J. Jara Fornerod, J. Harberts, P.S. Zangabad, N.H. Voelcker, Wearable microneedle patch for transdermal electrochemical monitoring of urea in interstitial fluid, ACS Sens. 9 (2) (2024) 932, https://doi.org/10.1021/acssensors.3c02386.
[265] H. Liu, X. Zhou, A. Nail, H. Yu, Z. Yu, Y. Sun, K. Wang, N. Bao, D. Meng, L. Zhu, H. Li, Multi-material 3D printed eutectogel microneedle patches integrated with fast customization and tunable drug delivery, J. Contr. Release 368 (2024) 115, https://doi.org/10.1016/j.jconrel.2024.02.023.
[266] Chenthattil Raril, J.G. Manjunatha, D.K. Ravishankar, S. Fattepur, G. Siddaraju, L. Nanjundaswamy, Validated electrochemical method for simultaneous resolution of tyrosine, uric acid, and ascorbic acid at polymer modified nano-composite paste electrode, Surf. Eng. Appl. Electrochem. 56 (2020) 415, https://doi.org/10.3103/S1068375520040134.
[267] M.M. Charithra, J.G.G. Manjunatha, C. Raril, Surfactant modified graphite paste electrode as an electrochemical sensor for the enhanced voltammetric detection of estriol with dopamine and uric acid, Adv. Pharmaceut. Bull. 10 (2) (2020) 247, https://doi.org/10.34172/apb.2020.029.
[268] C. Raril, J.G. Manjunatha, G. Tigari, Low-cost voltammetric sensor based on an anionic surfactant modified carbon nanocomposite material for the rapid determination of curcumin in natural food supplement, Instrum. Sci. Technol. 48 (2020) 561, https://doi.org/10.1080/10739149.2020.1756317.
[269] G. Tigari, J.G. Manjunatha, Optimized voltammetric experiment for the determination of phloroglucinol at surfactant modified carbon nanotube paste electrode, Instrum. Exp. Tech. 63 (2020) 750, https://doi.org/10.1134/S0020441220050139.
[270] N. Sreeharsha, M. Telsang, G.M. Basavarajappa, S. Pund, R.K. Karnati, Poly (threonine) modified carbon composite electrode as sensor for amoxicillin determination, Int. J. Electrochem. Sci. 17 (2) (2022) 220229, https://doi.org/10.20964/2022.02.25.
[271] N. Hareesha, J.G. Manjunatha, C. Raril, G. Tigari, Sensitive and selective electrochemical resolution of tyrosine with ascorbic acid through the development of electropolymerized alizarin sodium sulfonate modified carbon nanotube paste electrodes, ChemistrySelect 4 (2019) 4559, https://doi.org/10.1002/slct.201900794.
[272] M. Parrilla, U. Detamornrat, J. Domínguez-Robles, R.F. Donnelly, K. De Wael, Wearable hollow microneedle sensing patches for the transdermal electrochemical monitoring of glucose, Talanta 249 (2022) 123695, https://doi.org/10.1016/j.talanta.2022.123695.
[273] M. Reynoso, A.Y. Chang, Y. Wu, R. Murray, S. Suresh, Y. Dugas, J. Wang, N. Arroyo-Currás, 3D-printed, aptamer-based microneedle sensor arrays using magnetic placement on live rats for pharmacokinetic measurements in interstitial fluid, Biosens. Bioelectron. 244 (2024) 115802, https://doi.org/10.1016/j.bios.2023.115802.
[274] V.M. Vaz, L. Kumar, 3D printing as a promising tool in personalized medicine, AAPS PharmSciTech 22 (49) (2021), https://doi.org/10.1208/s12249-020-01905-8.
[275] M. Olowe, S.K. Parupelli, S. Desai, A review of 3D-printing of microneedles, Pharmaceutics 14 (12) (2022) 2693, https://doi.org/10.3390/pharmaceutics14122693.
[276] M.A. Ali, C. Hu, E.A. Yttri, R. Panat, Recent advances in 3D printing of biomedical sensing devices, Adv. Funct. Mater. 32 (9) (2022) 21076711, https://doi.org/10.1002/adfm.202107671.
[277] X. Yuan, O. Ouaskioud, X. Yin, C. Li, P. Ma, Y. Yang, P.F. Yang, L. Xie, L. Ren, Epidermal wearable biosensors for the continuous monitoring of biomarkers of chronic disease in interstitial fluid, Micromachines 14 (7) (2023) 1452, https://doi.org/10.3390/mi14071452.
[278] S. Lin, X. Cheng, J. Zhu, B. Wang, D. Jelinek, Y. Zhao, T.-Y. Wu, A. Horrillo, J. Tan, J. Yeung, W. Yan, S. Forman, H.A. Coller, C. Milla, S. Emaminejad, Wearable microneedle-based electrochemical aptamer biosensing for precision dosing of drugs with narrow therapeutic windows, Sci. Adv. 8 (38) (2022) eabq4539, https://doi.org/10.1126/sciadv.abq4539.
[279] Q. Duan, W.C. Zhang, J. Liu, F. Jin, X.Z. Dong, F.C. Bin, P. Steinbauer, E. Zerobin, M. Guo, T. Li, S. Baudis, M.L. Zheng, 22 nm resolution achieved by femtosecond laser two-photon polymerization of a hyaluronic acid vinyl ester hydrogel, ACS Appl. Mater. Interfaces 15 (22) (2023) 26472, https://doi.org/10.1021/acsami.3c04346.
[280] L. Antonara, P.P. Dallas, D.M. Rekkas, A novel 3D printing enabled method for fast and reliable construction of polymeric microneedles using experimental design, J. Drug Deliv. Sci. Technol. 68 (2022) 102888, https://doi.org/10.1016/j.jddst.2021.102888.
[281] S.F. Iftekar, A. Aabid, A. Amir, M. Baig, Advancements and limitations in 3D printing materials and technologies: a critical review, Polymers 15 (11) (2023) 2519, https://doi.org/10.3390/polym15112519.
[282] S. Bhatnagar, P.R. Gadeela, P. Thathireddy, V.V.K. Venuganti, Microneedle-based drug delivery: materials of construction, J. Chem. Sci. 131 (2019) 1–28, https://doi.org/10.1007/s12039-019-1666-x.
[283] Y. Xie, J. He, W. He, T. Iftikhar, C. Zhang, L. Su, X. Zhang, Enhanced interstitial fluid extraction and rapid analysis via vacuum tube-integrated microneedle array device, Adv. Sci. 11 (21) (2024) 2308716, https://doi.org/10.1002/advs.202308716.
[284] M. Dervisevic, J. Harberts, R. Sánchez-Salcedo, N.H. Voelcker, 3D polymeric lattice microstructure-based microneedle array for transdermal electrochemical biosensing, Adv. Mater. 36 (48) (2024) 2412999, https://doi.org/10.1002/adma.202412999.
[285] A. Keirouz, Y.L. Mustafa, J.G. Turner, E. Lay, U. Jungwirth, F. Marken, H.S. Leese, Conductive polymer-coated 3D printed microneedles: biocompatible platforms for minimally invasive biosensing interfaces, Small 19 (14) (2023) 2206301, https://doi.org/10.1002/smll.202206301.
[286] Food and Agriculture Organization, How to feed the world in 2050, Roma, https://doi.org/10.1111/j.1728-4457.2009.00312.x, 2009.
[287] M. Ray, A. Ray, S. Dash, A. Mishra, K.G. Achary, S. Nayak, S. Singh, Fungal disease detection in plants: traditional assays, novel diagnostic techniques and biosensors, Biosens. Bioelectron. 87 (2017) 708, https://doi.org/10.1016/j.bios.2016.09.032.
[288] D. Moore, G.D. Robson, A.P.J. Trinci, 21st Century Guidebook to Fungi, second ed., 2020. https://www.cambridge.org/gb/academic/subjects/life-sciences/plant-science/21st-century-guidebook-fungi-2nd-edition. (Accessed 9 July 2020).
[289] FAO, New Standards to Curb the Global Spread of Plant Pests and Diseases, 2019. https://www.fao.org/newsroom/detail/New-standards-to-curb-the-global-spread-of-plant-pests-and-diseases/en. (Accessed 21 October 2024).
[290] R.M. Cardoso, T.S. Pereira, M.H.M. Facure, D.M. dos Santos, L.A. Mercante, L.H.C. Mattoso, D.S. Correa, Current progress in plant pathogen detection enabled by nanomaterials-based (bio)sensors, Sensors and Actuators Reports 4 (2022) 100068, https://doi.org/10.1016/J.SNR.2021.100068.
[291] D. Haloui, K. Oufaska, M. Oudani, K. El Yassini, Bridging industry 5.0 and agriculture 5.0: historical perspectives, opportunities, and future perspectives, Sustainability 2024 16 (9) (2024) 3507, https://doi.org/10.3390/SU16093507.
[292] Latief Ahmad, Firasath Nabi, Agriculture 5.0 : Artificial Intelligence, IoT and Machine Learning, CRC Press, 2021. https://www.routledge.com/Agriculture-50-Artificial-Intelligence-IoT-and-Machine-Learning/Ahmad-Nabi/p/book/9780367646080. (Accessed 20 October 2024).
[293] A. Morchid, R. El Alami, A.A. Raezah, Y. Sabbar, Applications of internet of things (IoT) and sensors technology to increase food security and agricultural Sustainability: benefits and challenges, Ain Shams Eng. J. 15 (2024) 102509, https://doi.org/10.1016/J.ASEJ.2023.102509.
[294] N. Singh, A.N. Singh, Odysseys of agriculture sensors: current challenges and forthcoming prospects, Comput. Electron. Agric. 171 (2020) 105328, https://doi.org/10.1016/J.COMPAG.2020.105328.
[295] K. Berger, M. Machwitz, M. Kycko, S.C. Kefauver, S. Van Wittenberghe, M. Gerhards, J. Verrelst, C. Atzberger, C. van der Tol, A. Damm, U. Rascher, I. Herrmann, V.S. Paz, S. Fahrner, R. Pieruschka, E. Prikaziuk, M.L. Buchaillot, A. Halabuk, M. Celesti, G. Koren, E.T. Gormus, M. Rossini, M. Foerster, B. Siegmann, A. Abdelbaki, G. Tagliabue, T. Hank, R. Darvishzadeh, H. Aasen, M. Garcia, I. Pôças, S. Bandopadhyay, M. Sulis, E. Tomelleri, O. Rozenstein,

L. Filchev, G. Stancile, M. Schlerf, Multi-sensor spectral synergies for crop stress detection and monitoring in the optical domain: a review, Remote Sens. Environ. 280 (2022) 113198, https://doi.org/10.1016/J.RSE.2022.113198.

[296] R.F. Evert, S.E. Eichhorn, Raven biology of plants. https://doi.org/10.1007/978-1-319-15626-8, 2013.

[297] G. Dufil, I. Bernacka-Wojcik, A. Armada-Moreira, E. Stavrinidou, Plant bioelectronics and biohybrids: the growing contribution of organic electronic and carbon-based materials, Chem. Rev. 122 (4) (2022) 4847, https://doi.org/10.1021/acs.chemrev.1c00525.

[298] M. Parrilla, A. Sena-Torralba, A. Steijlen, S. Morais, Á. Maquieira, K. De Wael, A 3D-printed hollow microneedle-based electrochemical sensing device for in situ plant health monitoring, Biosens. Bioelectron. 251 (2024) 116131, https://doi.org/10.1016/J.BIOS.2024.116131.

[299] A. Bukhamsin, K. Moussi, R. Tao, G. Lubineau, I. Blilou, K.N. Salama, J. Kosel, Robust, long-term, and exceptionally sensitive microneedle-based bioimpedance sensor for precision farming, Adv. Sci. 8 (16) (2021) 2101261, https://doi.org/10.1002/advs.202101261.

[300] A. Varma, H. Padh, N. Shrivastava, Plant genomic DNA isolation: an art or a science, Biotechnol. J. 2 (2007) 386, https://doi.org/10.1002/BIOT.200600195.

[301] A. Bukhamsin, K. Moussi, N. Patel, A. Przybysz, Y. Wang, S. Krattinger, J. Kosel, Impedimetric plant biosensor based on minimally invasive and flexible microneedle electrodes, in: 2020 IEEE 33rd International Conference on Micro Electro Mechanical Systems (MEMS), IEEE, 2020, pp. 307–310, https://doi.org/10.1109/MEMS46641.2020.9056158.

[302] L. Santra, A. Kundu, S. Rajaraman, A flexible, digital light processing (DLP) 3D printed and coated microneedle array (CμNA) for precision delivery of novel nanotherapeutics to plant tissue. Proceedings of the IEEE International Conference on Micro Electro Mechanical Systems (MEMS) 2021-January, 2021, pp. 630–633, https://doi.org/10.1109/MEMS51782.2021.9375404.

[303] M. Parrilla, A. Steijlen, R. Kerremans, J. Jacobs, L. den Haan, J. De Vreese, Y. Van Noten Géron, P. Clerx, R. Watts, K. De Wael, Wearable platform based on 3D-printed solid microneedle potentiometric pH sensor for plant monitoring, Chem. Eng. J. 500 (2024) 157254, https://doi.org/10.1016/j.cej.2024.157254.

[304] H. Chen, S. Zhou, J. Chen, J. Zhou, K. Fan, Y. Pan, J. Ping, An integrated plant glucose monitoring system based on microneedle-enabled electrochemical sensor, Biosens. Bioelectron. 248 (2024) 115964, https://doi.org/10.1016/j.bios.2023.115964.

[305] M. Di Prima, J. Coburn, D. Hwang, J. Kelly, A. Khairuzzaman, L. Ricles, Additively manufactured medical products – the FDA perspective, 3D Print Med 2 (2016) 1, https://doi.org/10.1186/s41205-016-0005-9.